CCI Land Surface Temperature

Climate Assessment Report

WP5.1 – DEL-CAR

Ref.: LST-CCI-D5.1-CAR
Date: 17-Dec-2020
Organisation: Consortium CCI LST

Signatures

	Name	Organisation	Signature
Written by	Lizzie Good, Freya Aldred	Met Office	
	Ruth Mottram, Jacob Høyer	DMI	
	Panagiotis Sismanidis, Benjamin Bechtel	RUB	
	Sophia Walther	MPI-BGC	
	Sorin Cheval, Alexandru Dumitrescu	MeteoRomania	
	Kaniska Mallick, Christian Bossung	LIST	
	Debbie Hemming, Rob King	Met Office	
	Raquel Niclòs	University of Valencia	
Reviewed by	Darren Ghent	ULeic	
Approved by	Darren Ghent	ULeic	
Authorized by	Simon Pinnock	ESA	

Change log

Version	Date	Changes
1.0		First version

List of Changes

Version	Section	Changes

Table of Content

List of Figures

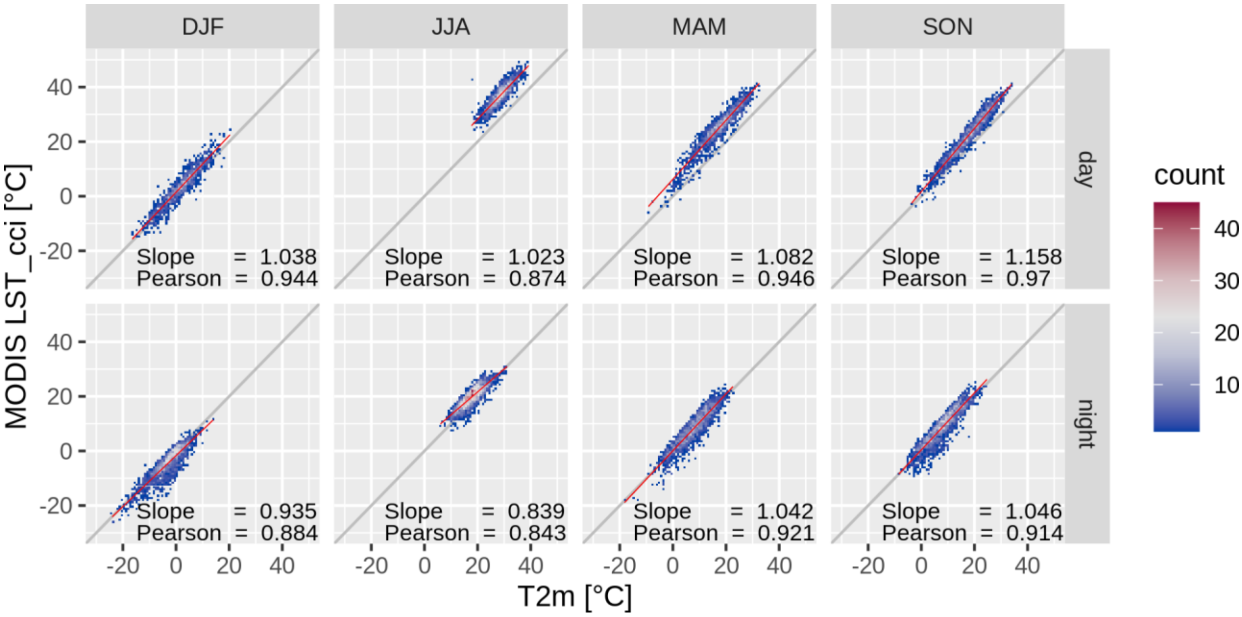
DJF
JJA
MAM
SON
day
night
count
MODIS LST_cci [°C]
T2m [°C]
Slope = 1.038
Pearson = 0.944
Slope = 1.023
Pearson = 0.874
Slope = 1.082
Pearson = 0.946
Slope = 1.158
Pearson = 0.97
Slope = 0.935
Pearson = 0.884
Slope = 0.839
Pearson = 0.843
Slope = 1.042
Pearson = 0.921
Slope = 1.046
Pearson = 0.914

List of Tables

Reference Documents

Identity	Reference
RD-01	Squintu, A.A.; van der Schrier, G.; van den Besselaar, E.J.M. (2019): EUSTACE / ECA&D: European land station daily air temperature measurements, homogenised. European Climate Assessment & Dataset, date of citation. https://catalogue.ceda.ac.uk/uuid/81784e3642bd465aa69c7fd40ffe1b1b
RD-02	Sen, P. K. (1968), Estimates of the regression coefficient based on Kendall's tau, J. Am. Stat. Assoc., 63, 1379–1389.
RD-03	Good, E. J., D. J. Ghent, C. E. Bulgin, and J. J. Remedios (2017), A spatiotemporal analysis of the relationship between near-surface air temperature and satellite land surface temperatures using 17 years of data from the ATSR series, J. Geophys. Res. Atmos., 122, 9185–9210, doi:10.1002/2017JD026880
RD-04	Vandecrux, B., Mottram, R., Langen, P. L., Fausto, R. S., Olesen, M., Stevens, C. M., Verjans, V., Leeson, A., Ligtenberg, S., Kuipers Munneke, P., Marchenko, S., van Pelt, W., Meyer, C. R., Simonsen, S. B., Heilig, A., Samimi, S., Marshall, S., Machguth, H., MacFerrin, M., Niwano, M., Miller, O., Voss, C. I., and Box, J. E.: The firn meltwater Retention Model Intercomparison Project (RetMIP): evaluation of nine firn models at four weather station sites on the Greenland ice sheet, The Cryosphere, 14, 3785–3810, https://doi.org/10.5194/tc-14-3785-2020, 2020.
RD-05	Fausto, R., van As, D., Box, J., Colgan, W. and Langen, P.: Quantifying the surface energy fluxes in South Greenland during the 2012 high melt episodes using in-situ observations, Frontiers in Earth Science, 4, 82, doi:10.3389/feart.2016.00082, 2016.
RD-06	Dybkjaer, G., Eastwood, S., Tonboe, R. T., Høyer, J., Borg, A. L., Englyst, P. N., ... & Jensen, M. B. (2018). Arctic and Antarctic ice Surface Temperatures from AVHRR thermal Infrared satellite sensors, 1982-2015. AGUFM, 2018, GC24C-01.
RD-07	Høyer, J. L., & Karagali, I. (2016). Sea surface temperature climate data record for the North Sea and Baltic Sea. Journal of Climate, 29(7), 2529-2541.
RD-08	Langen, P. L., Mottram, R. H., Christensen, J. H., Boberg, F., Rodehacke, C. B., Stendel, M., van As, D., Ahlstrøm, A. P., Mortensen, J., Rysgaard, S., Petersen, D., Svendsen, K. H., Aðalgeirsdóttir, G. and Cappelen, J.: Quantifying energy and mass fluxes controlling Godth\a absfjord freshwater input in a 5 km simulation (1991-2012), Journal of Climate, 28(9), 3694–3713, doi:10.1175/JCLI-D-14-00271.1, 2015.
RD-09	Langen, P. L., Fausto, R. S., Vandecrux, B., Mottram, R. H. and Box, J. E.: Liquid Water Flow and Retention on the Greenland Ice Sheet in the Regional Climate Model HIRHAM5: Local and Large-Scale Impacts, Frontiers in Earth Science, 4, doi:10.3389/feart.2016.00110, 2017.
RD-10	Mottram, R., Boberg, F., Lang Langen, P., Yang, S., Rodehacke, C., Christensen, J. and Madsen, M.: Surface Mass balance of the Greenland ice Sheet in the Regional Climate Model HIRHAM5: Present State and Future Prospects, , 75, 105–115, doi:10.14943/lowtemsci.75.105, 2017.
RD-11	Nielsen-Englyst, P., Høyer, J. L., Madsen, K. S., Tonboe, R. T., & Dybkjær, G. (2019a). Deriving Arctic 2 m air temperatures over snow and ice from satellite surface temperature measurements. The Cryosphere Discussions, 1-31.
RD-12	Nielsen-Englyst, P., Høyer, J. L., Madsen, K. S., Tonboe, R., Dybkjær, G., & Alerskans, E. (2019b). In situ observed relationships between snow and ice surface skin temperatures and 2 m air temperatures in the Arctic. Cryosphere, 13(3), 1005-1024.

Identity	Reference
RD-13	Kurtz, N., Richter-Menge, J., Farrell, S., Studinger, M., Paden, J., Sonntag, J., & Yungel, J. (2013). IceBridge airborne survey data support Arctic sea ice predictions. Eos, Transactions American Geophysical Union, 94(4), 41-41.
RD-14	Høyer, J. L., Le Borgne, P., & Eastwood, S. (2014). A bias correction method for Arctic satellite sea surface temperature observations. Remote Sensing of Environment, 146, 201-213.
RD-15	Manoli, G., Fatichi, S., Bou-Zeid, E., & Katul, G. G. (2020). Seasonal hysteresis of surface urban heat islands. Proceedings of the National Academy of Sciences, 117(13), 7082–7089. https://doi.org/10.1073/pnas.1917554117
RD-16	Zhou, B., Rybski, D., & Kropp, J. P. (2013). On the statistics of urban heat island intensity. Geophysical Research Letters, 40(20), 5486–5491. https://doi.org/10.1002/2013GL057320
RD-17	Jung, M., C. Schwalm, M. Migliavacca, S. Walther, G. Camps-Valls, et al. (2020), Scaling carbon fluxes from eddy covariance sites to globe: synthesis and evaluation of the FLUXCOM approach, Biogeosciences, 17, 1343–1365, https://doi.org/10.5194/bg-17-1343-2020
RD-18	Papale, D., M. Reichstein, M. Aubinet, E. Canfora, C. Bernhofer, et al.(2006), Towards a standardized processing of Net Ecosystem Exchange measured with eddy covariance technique: algorithms and uncertainty estimation, Biogeosciences, 3, 571–583, https://doi.org/10.5194/bg-3-571-2006.
RD-19	Ermida, S. L., I. F. Trigo, C. C. DaCamara, A. C. Pires (2018), A Methodology to Simulate LST Directional Effects Based on Parametric Models and Landscape Properties, Remote Sensing, 10, 1114; doi:10.3390/rs10071114.
RD-20	Oke, T. (1973), City Size and the Urban Heat Island, Atmos. Environ., 7, 769-779, doi:10.1016/0004-6981(73)90140-6.
RD-21	Millard, S.P. (2013), EnvStats: An R Package for Environmental Statistics. Springer, New York. ISBN 978-1-4614-8455-4
RD-22	USEPA. (2006), Data Quality Assessment: A Reviewer's Guide. EPA QA/G-9R. EPA/240/B-06/002, February 2006. Office of Environmental Information, U.S. Environmental Protection Agency, Washington, D.C.
RD-23	Rosner, B. (1975), On the Detection of Many Outliers. Technometrics 17, 221–227.
RD-24	Mallick, K., Jarvis, A. J., Boegh, E., Fisher, J. B., Drewry, D. T., Tu, K. P., Hook, S. J., Hulley, G., Ardo, J., Beringer, J., Arain, A., and Niyogi, D.: A Surface Temperature Initiated Closure (STIC) for surface energy balance fluxes, Remote Sens. Environ., 141, 243–261, https://doi.org/10.1016/j.rse.2013.10.022, 2014.
RD-25	Mallick, K., Boegh, E., Trebs, I., Alfieri, J. G., Kustas, W. P., Prueger, J. H., Niyogi, D., Das, N., Drewry, D. T., Hoffmann, L., and Jarvis, A. J.: Reintroducing radiometric surface temperature into the Penman–Monteith formulation, Water Resour. Res., 51, 6214–6243, https://doi.org/10.1002/2014wr016106, 2015.
RD-26	Mallick, K., Trebs, I., Boegh, E., Giustarini, L., Schlerf, M., Drewry, D. T., Hoffmann, L., von Randow, C., Kruijt, B., Araùjo, A., Saleska, S., Ehleringer, J. R., Domingues, T. F., Ometto, J. P. H. B., Nobre, A. D., de Moraes, O. L. L., Hayek, M., Munger, J. W., and Wofsy, S. C.: Canopy-scale biophysical controls of transpiration and evaporation in the Amazon Basin, Hydrol. Earth Syst. Sci., 20, 4237–4264, https://doi.org/10.5194/hess-20-4237-2016, 2016.
RD-27	Mallick K, Toivonen E, Trebs I, Boegh E, Cleverly J, Eamus D, Koivusalo H, Drewry D, Arndt SK, Griebel A, Beringer J, and Garcia M (2018): Bridging Thermal Infrared Sensing and Physically-Based Evapotranspiration Modeling: From Theoretical Implementation to

Identity	Reference
	Validation Across an Aridity Gradient in Australian Ecosystems, Water Resources Research, 54, 3409–3435. https://doi.org/10.1029/2017WR021357 (open access).
RD-28	Gowik, U., and P. Westhoff (2011), The Path from C3 to C4 Photosynthesis, Plant Phys., 155(1), 56-63, doi:10.1104/pp.110.165308.
RD-29	Coll, C., Caselles, V., Galve, J.M., Valor, E., Niclòs, R., Sánchez, J.M., Rivas, R. (2005). Ground measurements for the validation of land surface temperatures derived from AATSR and MODIS data. Rem. Sens. Environ. 97, 288–300.
RD-30	Niclòs, R., Pérez-Planells, Ll., Valiente, J.A., Coll, C., Valor, E., 2018. Evaluation of the S-NPP VIIRS Land Surface Temperature product using ground data acquired by an autonomous system at a rice paddy. ISPRS J. Photogramm. Remote Sens. 135, 1-12.
RD-31	Wan, Z., Dozier, J., 1996. A generalized split-window algorithm for retrieving land-surface temperature from space. IEEE Trans. Geosci. Remote Sens. 34, 892–905.
RD-32	Wan, Z., 2014. New refinements and validation of the collection-6 MODIS land-surface temperature/emissivity product. Remote Sens. Environ. 140, 36–45.
RD-33	Gillespie, A.R., Matsunaga, T., Rokugawa, S., Hook, S.J., 1998. Temperature and emissivity separation from Advanced Spaceborne Thermal Emission and Reflection Radiometer (ASTER) images. IEEE Trans. Geosci. Rem. Sens. 36, 1113–1125.
RD-34	Hulley, G. C., S. J. Hook, and A. M. Baldridge (2011), Generating consistent land surface temperature and emissivity products between ASTER and MODIS data for Earth science research, IEEE Trans. Geosci. Remote Sens., 49(4), 1304–1315, doi:10.1109/TGRS.2010.2063034.
RD-35	Coll, C., Niclòs, R., Puchades, J., García-Santos, V., Galve, J.M., Pérez-Planells, Ll., Valor, E., Theocharous, E. (2019). Laboratory calibration and field measurement of land surface temperatura and emissivity using thermal infrared multiband radiometers. Int. J. Appl. Earth Obs. Geoinformation, 78, 227-239.
RD-36	Theocharous, E., N. P. Fox , I. Barker-Snook , R. Niclòs, V. Garcia Santos, P. J. Minnett, F. M. Göttsche, L. Poutier, N. Morgan , T. Nightingale, W. Wimmer, J. Høyer , K. Zhang , M. Yang , L. Guan, M. Arbelo, and C. J. Donlon (2019). The 2016 CEOS Infrared Radiometer Comparison: Part II: Laboratory Comparison of Radiation Thermometers. Journal of Atmospheric and Oceanic Technology, 1079–1092. 10.1175/JTECH-D-18-0032.1.
RD-37	Guillevic, P., Göttsche, F., Nickeson, J., Hulley, G., Ghent, D., Yu, Y., Trigo, I., Hook, S., Sobrino, J.A., Remedios, J., Román, M., Camacho, F. (2018). Land surface temperature product validation best practice protocol version 1.1. Best Pract. Satell. L. Prod. Valid. (p. 60) L. Prod. Valid. Subgr. doi, 58. https://doi.org/10.5067/doc/ceoswgcv/lpv/lst.001.
RD-38	Hulley, G.C., Hook, S.J., 2009. The North American ASTER Land Surface Emissivity Database (NAALSED). Version 2.0. Remote Sens. Environ., 113, 1967–1975.
RD-39	Good, E. (2016), An in situ-based analysis of the relationship between land surface 'skin' and screen-level air temperatures, J. Geophys. Res. Atmos., 121, 8801–8819, doi:10.1002/2016JD025318.
RD-40	LST_cci (2020) Algorithm Development Plan, Reference LST-CCI-D2.4-ADP v2

Executive Summary

This document represents the first Climate Assessment Report (CAR) for the LST_cci project (https://climate.esa.int/en/projects/land-surface-temperature/). It comprises of reports from the six dedicated LST_cci project User Case Studies (UCS) and reports from other studies that have used beta versions of the LST_cci data sets produced during the first two years of the project. None of the studies are complete, but the early feedback collected here is made available to the LST_cci Science Team to further develop and improve the LST_cci data sets and plan for the next phases of the project.

The overall user feedback on the beta LST_cci products is generally very positive:

- In general, users report the products are easy to use and are well described in netCDF format. Users comment that the common format for LST products from different sensors is very valuable.

- Users appreciate the provision of additional fields in the files, such as viewing and solar geometry, and land cover class.

- Several of the studies reported here use Level 3 0.01° LST data; the provision of these higher-resolution data has been core to the success of these studies so far.

- The Level 3C (L3C) LST products are generally well correlated with collocated 2-m air temperatures (T2m) for both 'actual' and 'anomaly' temperatures.

- The Surface Urban Heat Island Intensity (SUHII) estimates and hysteretic cycles calculated from the 0.01° LST_cci custom products agree with those reported in the published literature using other products.

A number of issues that affect the utility of these data sets for climate applications have been identified by these early users. Many of these issues are already being addressed by the Science Team and will be implemented in the v2.0 release. The main issues identified include:

- Non-climatic discontinuities in the multi-sensor infrared (IR) and microwave (MW) products
    - Improvements are currently being made in both cases to improve the homogeneity of the data sets by improving intercalibration and overpass time corrections.

- Issues relating to the averaging method used to create the L3 IR products where data are averaged over several orbits/timestamps that affects the utility of the data, particularly at high latitudes
    - A new approach is being implemented for the LST_cci v2.0 products where the observation closest to the nominal overpass time of the sensor will be used to resolve this issue.

- Likely cold biases in the MODIS retrievals over the Greenland ice sheet but warm biases over a test site in Spain.

- This is primarily due to the LST_cci v1.0 products using an older emissivity data set. The LST_cci v2.0 products will use an improved data set, which is expected to resolve many of these 'bias' issues.

- Residual cloud contamination in the IR data sets (severe for some data sets)
  - Some of this cloud contamination is due to bug in the processor, which has now been resolved. Cloud masking will also be improved in the LST_cci v2.0 products through the use of a probabilistic cloud detection scheme.

- Difficulty in using the LST_cci 0.01° data due to the way the data are delivered to users
  - Improved delivery of the 0.01° data is currently being investigated by the Science Team; a simple HxV system to identify the tiles according to their geolocation may be implemented.

In addition, several minor issues/errors within the LST_cci data files have also been identified, for example, errors in some of the attribute names, presenting static land cover rather dynamic information and differences between the quality and auxiliary information presented in the IR and MW data files. Regular communication between the Climate Research Group (CRG, which comprise the UCS and other users) and the Science Team has ensured that these issues have been resolved quickly.

A list of further recommendations or areas for development to be considered in future years of the LST_cci project is also presented in this report.

The User Case Studies have provided highly relevant feedback for the Science Team to improve the performance of the LST_cci products. The Science Team have in parallel been working on improvements to these products for the next data version (v2.00) and have taken on board feedback from the CRG throughout the progress of the User Case Studies. While the focus of this report is on an independent climate assessment of the LST_cci products details information on the wider context of how the project is responding to the feedback is also provided.

1. Introduction

1.1 Purpose and scope

The European Space Agency's (ESA's) Climate Change Initiative (CCI) project aims to provide a comprehensive and timely response to the challenging requirements set by the Global Climate Observing System (GCOS) and the Committee on Earth Observation Satellites (CEOS) for highly stable, long-term, satellite-based products for climate research.

Space observations provide unique information that cannot be obtained from traditional ground stations – they can provide better spatial coverage and resolution, and records are now approaching the time periods required for climate research. As part of the CCI project, a total of 22 Essential Climate Variables (ECVs) have been targeted. Fourteen of these ECVs were included in the first phase of ESA's CCI project. A further eight have been selected for the second phase of the project, which includes Land Surface Temperature (LST). The LST_cci project aims to deliver a significant improvement on the capability of current satellite LST data records to meet the GCOS requirements for climate applications and realise the full potential of long-term LST data for climate science (https://climate.esa.int/en/projects/land-surface-temperature/).

Now in its third year, the LST_cci project has produced beta products for a range of satellites that include instruments operating at both infrared (IR) and microwave (MW) wavelengths, and in polar-orbiting and geostationary orbit (Table 1-1). These beta products were delivered just after the end of the first year of the project. They have been made available to selected users who are performing dedicated user case studies (UCS) that are funded through the LST_cci project, users from other CCI projects (e.g. permafrost_cci) and the CCI Climate Modelling User Group (CMUG), and other interested parties who are in direct contact with the LST_cci science team. Such trailblazer users are critical to the success of the project as they can provide early feedback and assessment of the LST_cci data sets that can be used to improve the products while they are being developed and before they are officially released to the wider public.

As ESA's CCI project targets the production of data sets that can be used for climate research, a crucial requirement is to assess the suitability and utility of these data from a climate-science perspective. Across CCI, this is performed through the Climate Assessment Reports (CAR) that are produced by each CCI project. This document presents the CAR version 1.0 (v1.0) for the LST_cci project. The objective of the report is to provide information on the suitability of the beta LST_cci data products for climate applications. This CAR focuses on both climate-critical aspects of the data, such as stability and homogeneity, and the utility and presentation of the data in a way that is useful for climate applications. The assessment is based on reports from the User Case Studies (UCS) funded through the LST_cci project and other studies that are not directly funded through the project.

1.2 Structure of the document

This document consists of three sections. Section 2 presents the reports from the six UCS that are funded through the LST_cci project, while Section 3 presents reports from other studies that have used the LST_cci beta products. For both sets of reports, the scientific objectives of the study are outlined together with a brief description of the study approach and results. Feedback on the utility of the LST_cci data from each study is also provided. Section 4 of the report synthesises the findings from all studies presented in Section 2 and Section 3 and summarises the main outcomes of this CAR.

1.3 Definition of terms

The terms used in this report are listed below, together with their definitions.

Term	Definition
AASTI	Arctic and Antarctic ice Surface Temperatures from thermal Infrared satellite sensors
AATSR	Advanced Along-Track Scanning Radiometer
ATSR	Along-Track Scanning Radiometer
ATSR-2	Second ATSR instrument
AVHRR	Advanced Very High Resolution Radiometer
C3	C3 Plant Functional Type
C4	C4 Plant Functional Type
CAR	Climate Assessment Report
CCI	Climate Change Initiative
CDR	Climate Data Record
CEOS	Committee on Earth Observation Satellites
CMIP6	Climate Model Intercomparison Project 6
CMUG	Climate Modelling User Group
CRG	Climate Research Group
DMI	Danmarks Meteorologiske Institut (Danish Meteorological Institute)
DMSP	Defense Meteorological Satellite Program
E	Evapotranspiration
E_E	Evaporation
E_T	Transpiration
EC	Eddy Covariance
ECV	Essential Climate Variable
EOS	Earth Observing System
ERA5	ECMWF Reanalysis 5
ERS-2	Second European Remote Sensing satellite
ESA	European Space Agency
ESM	Earth System Model
EUSTACE	EU Surface Temperature for All Corners of Earth
FCDR	Fundamental Climate Data Record
GCOS	Global Climate Observing System
H	Sensible heat flux
IPCC	Intergovernmental Panel on Climate Change

Term	**Definition**
IR	InfraRed
IST	Ice Surface Temperature
K	Kelvin
L3	Level 3
L4	Level 4
L3C	Level 3C
LC	Land Cover
LC_cci	Land Cover Climate Change Initiative
LCC	Land Cover Class
LE	Latent heat flux
LST	Land Surface Temperature
LIST	Luxemburg Institute of Science and Technology
LSA SAF	Satellite Application Facility on Land Surface Analysis
LST_cci	Land Surface Temperature Climate Change Initiative
m	Slope / gradient of a straight line
MeteoRomania	National Meteorological Administration of Romania
MODIS	Moderate Resolution Imaging Spectroradiometer
MOHC	Met Office Hadley Centre
MPI-BGC	Max Planck Institute for Biogeochemistry
MPW	Median of Pairwise Slopes
MSG	Meteosat Second Generation
MSLP	Mean Sea-Level Pressure
MW	MicroWave
NASA	National Aeronautics and Space Administration (USA)
NATT	North Australian Tropical Transect
netCDF	Network Common Data Format
NOAA	National Oceanic and Atmospheric Administration (USA)
PUG	Product User Guide
r	Pearson correlation coefficient
RCM	Regional Climate Model
RetMIP	Retention Model Intercomparison Project
RMS	Root Mean Square
RUB	Ruhr-University Bochum
S_T	Water stress

Term	Definition
SATAZ	Satellite Azimuth Angle
SATZE	Satellite Zenith Angle
SEB	Surface Energy Balance
SEVIRI	Spinning Enhanced Visible and Infra-Red Imager
SLSTR	Sea and Land Surface Temperature Radiometer
SM_cci	Soil Moisture Climate Change Initiative
SMB	Surface Mass Balance
SSM/I	Special Sensor Microwave/Imager
SSMIS	Special Sensor Microwave Imager Sounder
STIC	Surface Temperature Initiated Closure
SUHI	Surface Urban Heat Island
SUHII	Surface Urban Heat Island Intensity
T2m	2m air temperature
UCS	User Case Study
UKESM	UK Earth System Model
UHI	Urban Heat Island
WMO	World Meteorological Organisation

Table 1-1: LST_cci products (from List of Climate Data Research Package document v1.1).

Product String	Version	Instrument	LST_cci ID	Satellite	Spatial Resolution	Temporal Resolution	Data Availability	Data Accessibility (Workspace)
ERS-2_ATSR__L2P	1.00	ATSR-2	ATSR_2	ERS-2	1 km swath	Full orbit	1995 – 2003	Private (leicester)
ERS-2_ATSR__L3C					0.05° global lon-lat grid	Daily / Month – Day + Night		Public (esacci_lst)
ENVISAT_ATSR__L2P	1.00	AATSR	ATSR_3	Envisat	1 km swath	Full orbit	2002 – 2012	Private (leicester)
ENVISAT_ATSR__L3C					0.05° global lon-lat grid	Daily / Month – Day + Night		Public (esacci_lst)
TERRA_MODIS_L2P	1.00	MODIS	MODIST	EOS Terra	1 km swath	5 minute granules	2000 – 2018	Restricted (nceo_generic)
TERRA_MODIS_L3C					0.05° global lon-lat grid	Daily / Month – Day + Night		Public (esacci_lst)
AQUA_MODIS_L2P	1.00	MODIS	MODISA	EOS Aqua	1 km swath	5 minute granules	2002 – 2018	Restricted (nceo_generic)
AQUA_MODIS_L3C					0.05° global lon-lat grid	Daily / Month – Day + Night		Public (esacci_lst)
SENTINEL3A_SLSTR_L2P	1.00	SLSTR	SLSTRA	Sentinel 3A	1 km swath	3 minute granules	2016 – 2018	Private (leicester)
SENTINEL3A_SLSTR_L3C					0.05° global lon-lat grid	Daily / Month – Day + Night		Public (esacci_lst)
MSG_SEVIRI_L3U	1.01	SEVIRI	SEVCCI	Meteosat	0.05° regional lon-lat grid	Hourly	2008 – 2010	Public (esacci_lst)
SSMI_SSMIS_L3C	1.12	SSM/I + SSMIS	SSMI13 / SSMI17 / SSMI18	DMSP	0.25° global lon-lat grid	Daily – Ascending + Descending	1995 - 2018	Public (esacci_lst)
MULTISENSOR_IRCDR_L3S	1.00	ATSR-2 + AATSR	ATSR_2 / ATSR_3	ERS-2 + Envisat	0.05° global lon-lat grid	Daily / Month – Day + Night	1995 - 2012	Public (esacci_lst)

All Level-3C data can be accessed on the “Public” partition of the “esacci_lst” workspace on JASMIN through the link: http://gws-access.ceda.ac.uk/public/esacci_lst/

Data on the “Private” and “Restricted” (requires authorisation) workspaces are stored on these based entirely on data storage requirements for Level-2 data

2. Funded User Case Study Reports

2.1 Regional and Global Trends in LST: A Stability Assessment of the LST_cci Products (Met Office)

2.1.1 Key Messages

- The stability of all L3C and the MULTISENSOR_IRCDR_L3S LST_cci products is assessed to determine if they are sufficiently stable for climate trend detection
- The LST_cci datasets show good correlation with 2m air temperature records
- The current versions of multi-sensor products show non-climatic discontinuities between sensors and therefore cannot be used for trend analysis
- The LST_cci products are generally very useful and easy to use
- There are some minor issues with the data format (mistakes) and some possible cloud contamination in the MODIS data

2.1.2 Scientific Analysis

2.1.2.1 Aims of the study

Trends in 2m air temperature (T2m) are well established and are a key metric for understanding climate change. T2m observations are obtained from a network of weather stations across the globe, which can be sparse in some regions such as Africa and Greenland. This leads to gaps in the derived datasets and therefore larger uncertainties in the estimated trends. If sufficiently stable in time, satellite-observed Land Surface Temperatures (LST) provide useful complimentary observations now that multidecadal records are available. LST can provide independent information on changes in surface temperature where T2m observations exist and new information where T2m observations are unavailable.

The objective of this study is to determine whether temperature trends are present in the LST_cci products and to compare them with equivalent, known trends in T2m. Before this can be carried out, the temporal stability of the products is assessed to determine if climatic temperature trends can be reliably detected. The relationship between collocated LST_cci and homogenised T2m anomaly datasets is explored to assess the stability of the LST_cci data.

2.1.2.2 Data and Methods

The LST datasets used for this study are summarised in Table 2-1. All the InfraRed (IR) datasets are daily with separate fields for daytime (LST_{day}) and night-time (LST_{night}) overpasses for the IR products. The overpass time is different for each instrument, but this is stable for each IR instrument during its lifetime. For the multi-sensor product, which comprises ATSR-2 and AATSR, the overpass time for the ATSR-2 data (10:30 am/pm) has been corrected to overpass time of the AATSR (10:00 am/pm). The multi-sensor MW product is also daily, but with separate fields for ascending (LST_{asc}) and descending (LST_{desc}) overpasses, rather than daytime and nighttime due to the overpass time and orbital drift. Unlike for the IR instruments, the orbit for each MW instrument that comprises the data set drifts in time and this orbital drift is not corrected in the LST_cci dataset.

Table 2-1: A summary of LST_cci products used for this case study.

Product String	Sensor type	Resolution	Data availability	Local time of ascending node
ERS-2_ATSR__L3C	IR	0.05°	August 1995 – June 2003	22:30
ENVISAT_ATSR__L3C	IR	0.05°	July 2002 – April 2012	22:00
TERRA_MODIS_L3C	IR	0.05°	February 2000 – December 2018	22:30
AQUA_MODIS_L3C	IR	0.05°	July 2002 – December 2018	13:30
MULTISENSOR_IRCDR_L3S	IR	0.05°	August 1995 – March 2012	22:00 (ATSR-2 overpass time adjusted to AATSR)
SSMI_SSMIS_L3C	MW	0.25°	January 1995 – December 2018	Approximately 17:30-19:30

The stability of the LST_cci data sets is assessed using homogenised daily minimum ($T2m_{min}$) and maximum ($T2m_{max}$) T2m data provided by the EU Surface Temperature for All Corners of Earth (EUSTACE: https://www.eustaceproject.org/) for meteorological stations within Europe and the Mediterranean (RD-01). The gridded LST_cci products are spatially and temporally collocated with EUSTACE station locations. For the IR products, LST_{night} and LST_{day} are compared to $T2m_{min}$ and $T2m_{max}$ respectively. For the SSMI_SSMIS_L3C product, the LST_{desc} (~6-8 am) is compared to $T2m_{max}$ and LST_{asc} is compared to $T2m_{min}$; this will likely be changed in future analysis, or the focus will move to mean temperatures for this dataset.

Climatologies are calculated for the LST and T2m time series separately, for each station location, based on a 31-day moving median window calculated for each calendar day of the year. This is done for each of the satellite time periods so equivalent LST/T2m datasets can be compared. The median station climatology is then subtracted from the observed data to calculate the following anomaly time series:

Equation 2-1 $$LST_{day\_anom} = LST_{day\_observed} - LST_{day\_climatology}$$

Equation 2-2 $$LST_{night\_anom} = LST_{day\_observed} - LST_{day\_climatology}$$

Equation 2-3 $$LST_{desc\_anom} = LST_{desc\_observed} - LST_{desc\_climatology}$$

Equation 2-4 $$LST_{asc\_anom} = LST_{asc\_observed} - LST_{asc\_climatology}$$

Equation 2-5 $$T2m_{max\_anom} = T2m_{max\_observed} - T2m_{max\_climatology}$$

Equation 2-6 $$T2m_{min\_anom} = T2m_{min\_observed} - T2m_{min\_climatology}$$

The relationship between LST and T2m anomalies (LST anomaly vs T2m anomaly) is assessed at each station by calculating the Pearson correlation coefficient (r), and the slope (m) using the Median of PairWise (MPW) slopes (RD-02). A value of unity for both these parameters indicates a perfect relationship at that location.

To assess the stability of the products, monthly mean anomalies are calculated for LST and T2m using only temporally matched observations that are available in both datasets. A time series of differences is then calculated as:

Equation 2-7 $$Difference_{day\_anom} = LST_{day\_anom} - T2m_{max\_anom}$$

Equation 2-8 $$Difference_{night\_anom} = LST_{night\_anom} - T2m_{min\_anom}$$

Equation 2-9 $$Difference_{asc\_anom} = LST_{asc\_anom} - T2m_{min\_anom}$$

Equation 2-10 $$Difference_{desc\_anom} = LST_{desc\_anom} - T2m_{max\_anom}$$

Where the confidence interval of the slope of time series of differences does not encompass zero, the slope is considered to be statistically significant.

2.1.2.3 Results

The correlations and slopes for the relationship between LST and T2m anomalies at each station are generally around 0.7-0.8 for the MODIS Aqua and Terra data sets. However, both the correlations and slopes decrease with increasing latitude during the day (Figure 2-1). For the ATSR-2 and AATSR data sets, including the multi-sensor IR CDR, comparatively few matchups are obtained owing to the narrower swath, but correlations and slopes are generally lower than for MODIS, at around 0.5-0.7 (Figure 2-2). There are too few stations with matchups to determine whether there is any dependency with latitude. This latitude-dependent behaviour is not evident in the MW data set (not shown), where the correlations and slopes at each station appear stable with latitude ($r \approx 0.8$, $m \approx 0.8$). This apparent difference in behaviour between the MODIS and MW data sets is likely to be due to the way the data are averaged in the products. At high latitudes there can be multiple overpasses per day for each pixel as orbit overlap increases with increasing latitude. For the IR data sets the value for each grid cell has been produced by averaging all observations, which may be from multiple overpasses. By contrast, the MW data set uses those observations that are closest in time to the nominal overpass time of the satellite and does not average data from multiple orbits in a single grid cell. Averaging of the multiple orbits in the IR products therefore appears to create additional noise in the data, which is evidenced by the lower correlations and slopes that increasingly deviate from unity with increasing latitude.

The stability assessment of the multi-sensor products show that time series of LST and T2m monthly mean anomalies are generally consistent, as shown in the top row of Figure 2-3 (MULTISENSOR_IRCDR_L3S) and Figure 2-4 (SSMI_SSMIS_L3C). However, the differences shown in the bottom row of both figures suggest non-climatic discontinuities that correspond to changes in instrument. For the MULTISENSOR_IRCDR_L3S data, the ATSR-2 time series of differences is noisier compared with AATSR, which is reflected in the higher standard deviations for ATSR-2. This is particularly apparent for LST_{day}-$T2m_{max}$, where the standard deviation is 0.91 for ATSR-2 and 0.75 for AATSR. This is likely due to errors in the overpass time correction that has been applied to ATSR-2, evidenced by the larger differences in the standard deviations during the day, when this correction is more difficult. The SSMI_SSMIS_L3C product also exhibits discontinuities between instruments (Figure 2-4). For example, there is a very clear negative trend in the differences with time for LST_{desc}-$T2m_{max}$ for both DMSP-F13 and -F17 but there is a marked positive jump at the instrument transition. The trend in the differences then becomes positive for DMSP-F18. This is likely due to the change in overpass times between each sensor and the orbital drift, both of which are uncorrected in the current version of the data set. There are also notable differences in the variance for each sensor. This is reflected in the different standard deviations, which show the agreement with the T2m anomalies for DMSP-F18 is noisier than for the DMSP-F13 and -F17.

While there are no obvious jumps in the single-sensor time series, the slopes of the differenced anomaly time series are several $K decade^{-1}$ and are statistically different from zero for MODIS/Aqua LST_{night}-$T2m_{min}$ (Figure 2-5), MODIS/Terra LST_{night}-$T2m_{min}$ (not shown), AATSR LST_{night}-$T2m_{min}$ (not shown), and ATSR-2 LST_{day}-$T2m_{max}$ (not shown). This indicates that in these cases the slope of the LST anomaly time series is significantly different from the T2m anomaly time series. Possible reasons for the unexpected non-zero slopes of the anomaly differences include 1) the LST data are not homogeneous with time, 2) the trends in LST are different from the T2m trends, and 3) non-zero slopes are an artefact of the processing. Investigations into these non-zero slopes are ongoing but it should be noted that Good et al. (2017) [RD-03], who compared the GlobTemperature LST CDR with CRUTEM4 T2m data, concluded that trends in the LST-T2m differences were either statistically insignificant or very small (e.g. approximately -0.1 $K decade^{-1}$). However, it should be noted that T2m data used in this study and that of Good et al.

(2017) [RD-03] are not the same, although they should be very similar in principle. Another notable difference between the results of this study and that of Good et al. (2017) [RD-03] is that there is a prominent, unexpected annual cycle in the time series of differences in this study, which also requires further investigation (Figure 2-5).

2.1.2.4 Conclusions

In general, the collocated LST vs T2m station anomalies show reasonable correlations and slopes (r and m ≈ 0.6-0.8), which is encouraging in terms of the quality of LST_cci datasets and for the use of LST to complement T2m analyses in climate applications. However, analysis of L3 IR data above ~50° latitude should be approached with caution due to increased noise in the data at high latitudes, which is likely due to the averaging of data over overlapping overpasses.

The multi-sensor products show non-climatic discontinuities at sensor transitions, and the SSMI_SSMIS_L3C product displays a drift within the lifetime of each instrument. Therefore, the current versions of these datasets cannot be used for trend analysis. The single-sensor IR products appear to be free from any jumps, but the trends in these data do not agree with those in the T2m data, which requires further investigation and understanding before these data can be used for climate trend analysis.

2.1.3 Feedback on scientific utility of the LST_cci products

Generally, the LST_cci products have been easy to use, with a well described netCDF format. However there are some discrepancies in the format between the IR and MW products that makes analysis that uses both these types of products more challenging. The first is the difference in classification of day and night for IR data, and ascending and descending for MW data. This adds additional processing to read in the data when working with both data types. Secondly the two data types contain different variables in the files: a quality flag (‘qual_flag’) is provided with MW data but not IR data. The IR data is provided with a land water mask (‘lwm’) and number of cloudy pixels (‘ncld’) instead. The IR data also comes with the land cover class (‘lcc’) whilst the MW data does not. Whilst there is some sense to the differences, quality flags would certainly be useful with all data products, as would the land cover class and land water mask. Understandably the use of number of cloudy pixels is different for IR and MW data. The more consistent the format can be between products the easier they are to use in analyses.

In the MULTISENSOR_IRCDR_L3S product, some data files were found to have incorrect global attribute ‘platform’: where for ATSR_3 the platform should be Envisat, it is ERS-2, which can be identified by the purple dashed line in Figure 2-3. For the MODIS products (and possibly other products), the ‘standard_name’ field contents for both latitude and longitude is set to ‘latitude’.

Some anomalously low temperatures were identified, particularly in the MODIS datasets, which are thought to be due to cloud contamination. Whilst there are only a few there is no easy way to mask these values out during processing. It would be useful to have some guidance and further information on how best to handle this problem.

As discussed in Section 0, there is a difference in the way observations are averaged over a grid cell between IR and MW products. For the IR products, the grid cell value may be an average value from multiple orbits. This appears to make the IR products noisier than the MW product, which is reflected in the lower correlations between LST and T2m, and slopes that differ more substantially from unity, at high latitudes for IR datasets. It is therefore recommended that the IR products are produced using the approach that is currently used for the MW product, adopting the observation closest in time to the nominal overpass time of the sensor.

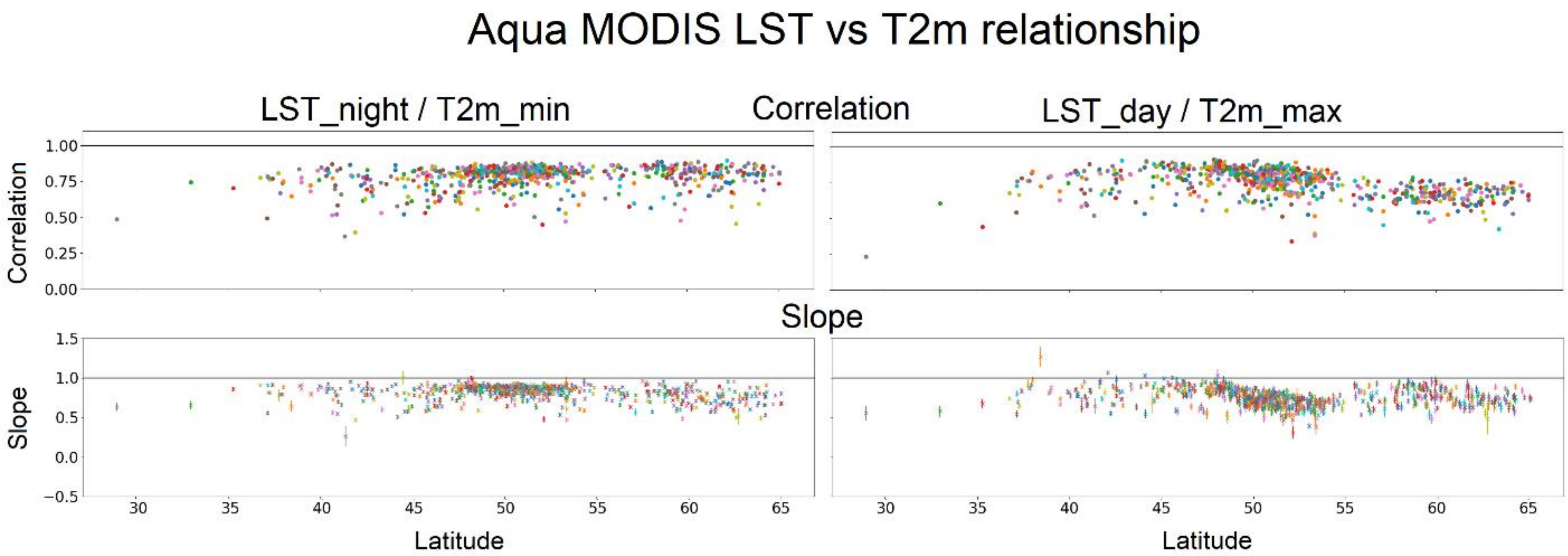

Figure 2-1: LST vs. T2m anomaly relationship correlation and slope for AQUA_MODIS_L3C v1.0. Each dot on the plot represents a different station location; the colours have no meaning and are only used to improve the clarity of the plot.

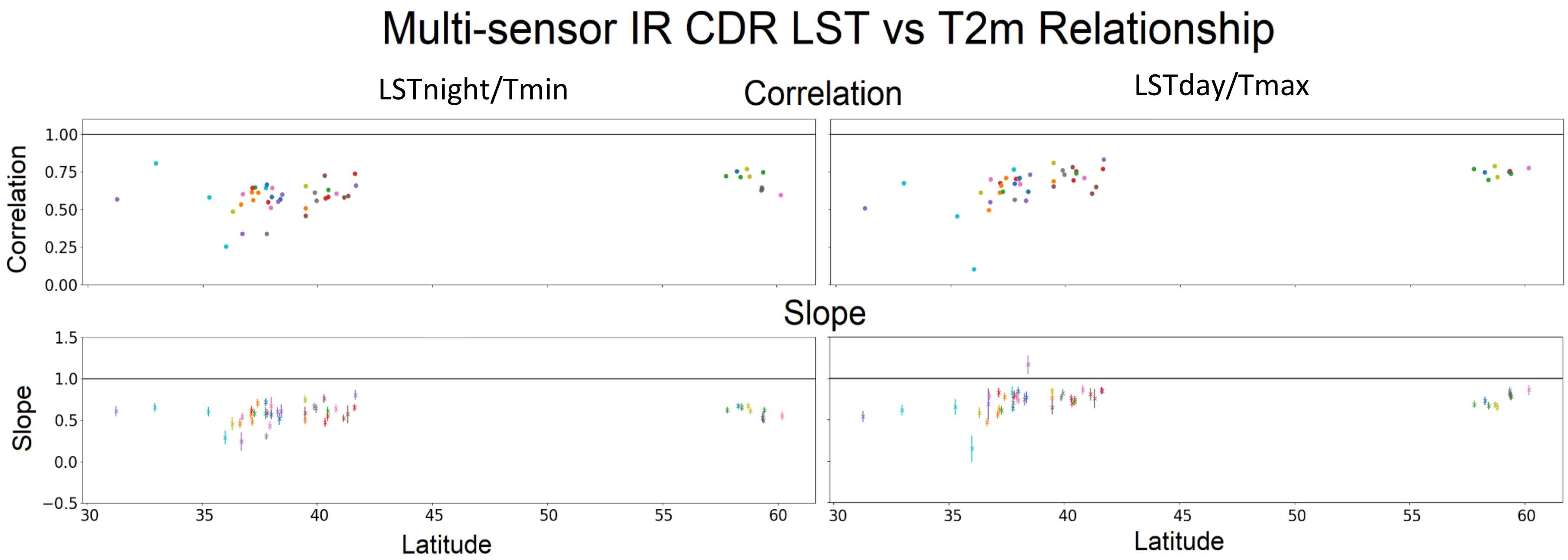

Figure 2-2: LST vs. T2m anomaly relationship correlation and slope for MULTISENSOR_IRCDR_L3S v1.0. Each dot on the plot represents a different station location; the colours have no meaning and are only used to improve the clarity of the plot.

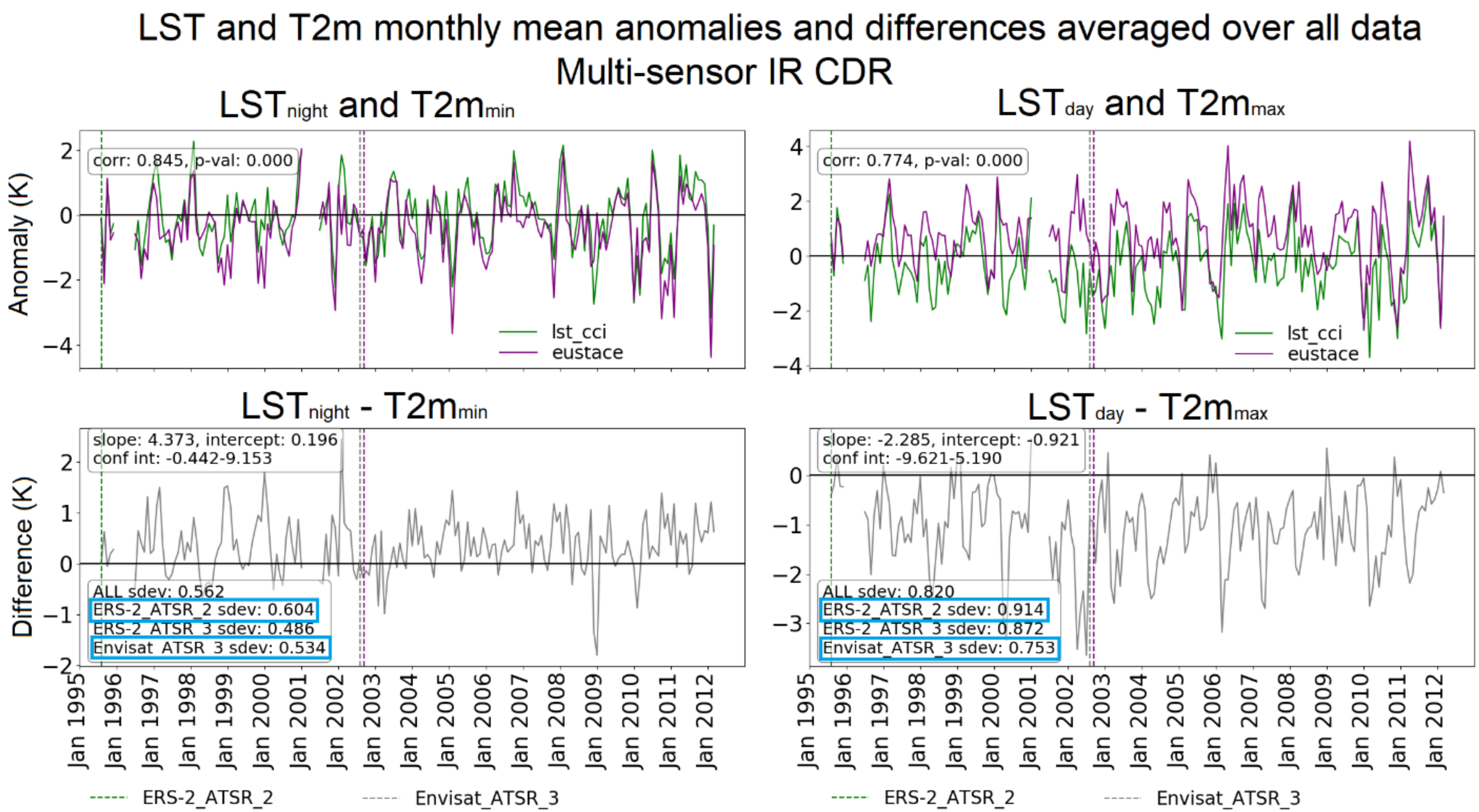

Figure 2-3: LST and T2m monthly mean anomalies (top) and LST-T2m differences (bottom) averaged over all available stations in Europe for MULTISENSOR_IRCDR_L3S v1.0. Sensor changeover between ATSR-2 and AATSR is plotted as the grey vertical dashed line.

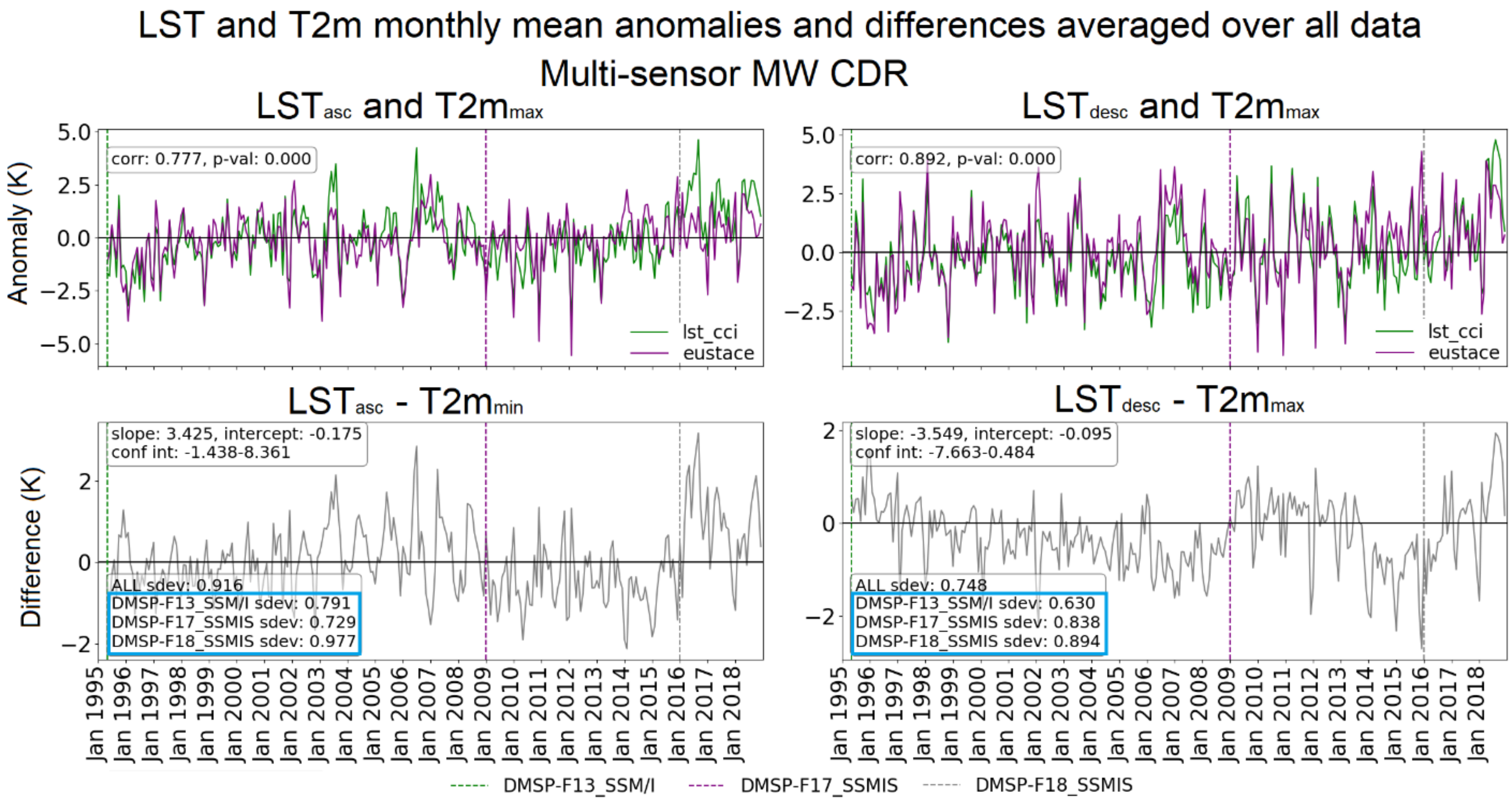

Figure 2-4: LST and T2m monthly mean anomalies (top) and LST-T2m differences (bottom) averaged over all available data in Europe for SSMI_SSMIS_L3C v1.12. Sensor changeovers are plotted as vertical dashed lines.

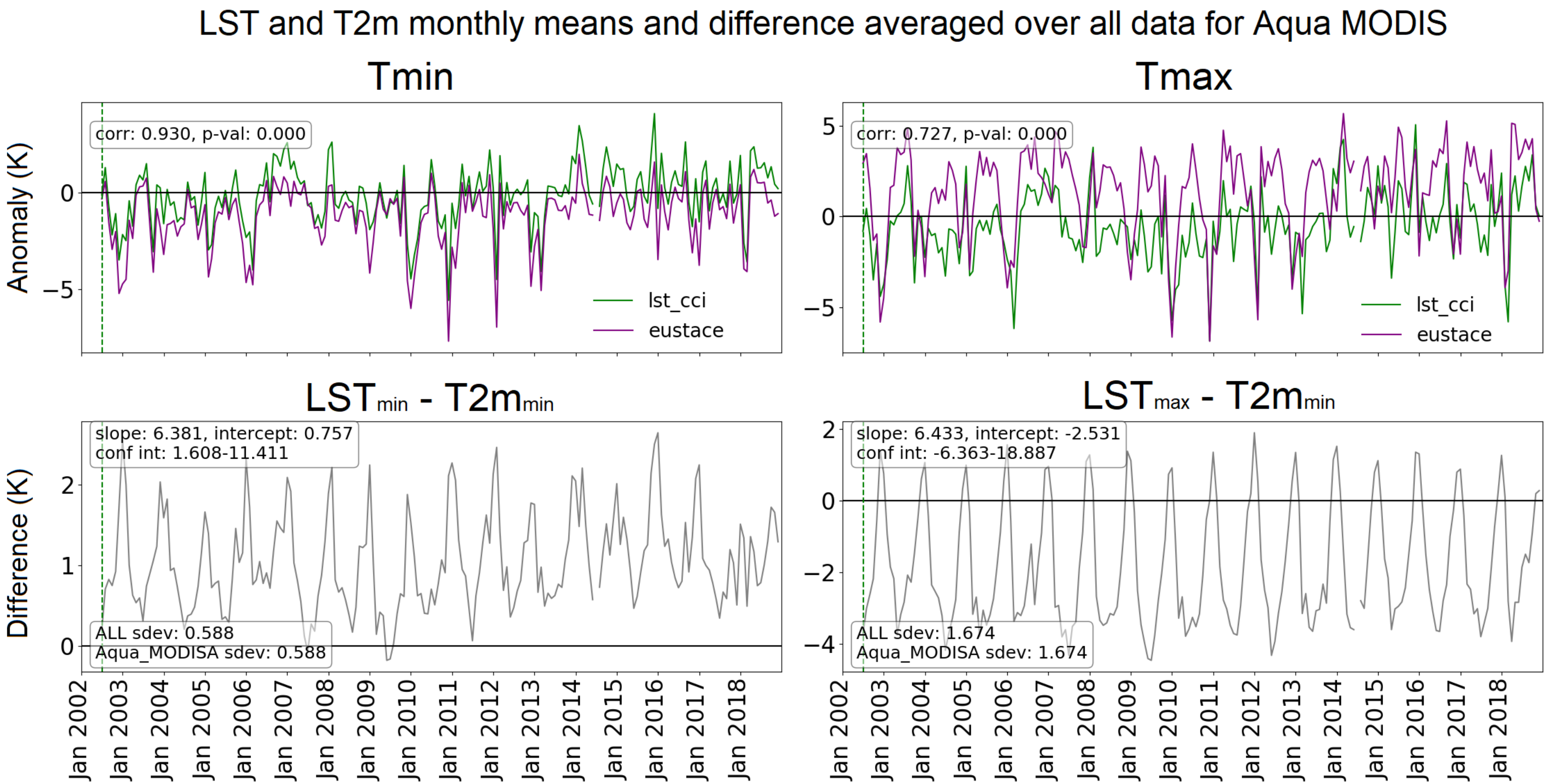

Figure 2-5: LST and T2m monthly mean anomalies (top) and LST-T2m differences (bottom) averaged over all available data in Europe for AQUA_MODIS_L3C v1.00.

Finally, as shown in Figure 2-3 and Figure 2-4, the multi-sensor products are not suitable for trend analysis due to the presence of significant non-climatic discontinuities. It is recommended that removal of these discontinuities is prioritised so that these data can be used reliably to detect trends.

2.2 Construction of a gap-free multisensor ice surface temperature product for the Greenland ice cap and assimilation into atmosphere and ice sheet models (DMI)

2.2.1 Key Messages

- High resolution Level 2 LST_cci products of Ice surface temperature (IST) from the Greenland ice sheet are used to construct a daily gap free level 4 Ice surface temperature product
- Data are evaluated against observations on the ice sheet and assimilated into a surface mass budget model of snow and firn processes for one year.
- The resulting L4 product performs satisfactorily in terms of quality when compared with surface temperature from IceBridge.

2.2.2 Scientific Analysis

2.2.2.1 Aims of the study

The aim of this study is to assess the use of satellite LST data products for improving model hindcasts of Greenland ice sheet surface mass budget. This requires that the high-resolution Level 2 LST_cci products of Ice surface temperature (IST) from the Greenland ice sheet are validated and used to construct a daily gap free level 4 IST product. As a pilot, the data products for the year 2012 will be assessed for use in combination with a regional climate model (RCM) and surface mass balance (SMB) model. For the pilot year, the performance of the RCM HIRHAM5 in calculating the surface energy budget over the Greenland ice sheet and determining the extent of surface melt will be assessed. The LST data will then also be integrated into a snow and firn (snow that has survived at least one annual cycle) SMB and run offline to assess the impact of including observational data to improve simulations of melt and retention. The protocol established in the Retention model intercomparison project (RetMIP) [RD-04] for evaluating improvements in the model system with data assimilation is adopted in this study.

The year 2012 has been chosen for this project. This was a year in which extensive surface melt covered most of the ice sheet, an event that occurred for the first time in the direct observational record. This was an important year with the lowest surface mass budget then in the record, but also a challenging one for climate models, many of which underestimated the contribution to melting of turbulent heat fluxes, especially the sensible heat flux [RD-05].

2.2.2.2 Data and Method

Due to the high latitudes of the Greenland ice sheets, it is not feasible to use aggregated day/night observations from ascending and descending orbits. Therefore, a special data package was made available for this UCS from the LST_cci project, consisting of the L2 1 km satellite IST observations from AATSR and MODIS. In addition, IST observations from the AASTI (Arctic and Antarctic ice Surface Temperatures from thermal Infrared satellite sensors) AVHRR GAC v2 data set provided by DMI and MET.NO, have been included in the analysis [RD-06]. The data satellite products used in this study are listed in Table 2-2.

Airborne radiometric surface temperature observations from the Icebridge project have been used to tune the statistical processing (e.g. temporal averaging window) and to validate the different satellite products. An example of the different satellite products is shown in the figure below, where the level 3 data fields are aggregated for a day and the Level 4 gap free product combines all data sources using a similar statistical methodology as in Høyer et al., (2016) [RD-07]. As evident from the figure, the sampling of the AATSR is more limited than for MODIS and AVHRR. Due to this sampling issue and the limited length of data (only part of the year 2012 is available) these data have not been used to generate the final Level 4 IST product.

Table 2-2: List of LST data sets used in the study

Product String	Sensor type	Resolution	Data availability
ENVISAT_ATSR__L2P	IR	1 km swath	Jan-April, 2012
TERRA_MODIS_L2P	IR	1 km swath	Jan-Dec, 2012
AQUA_MODIS_L2P	IR	1 km swath	Jan-Dec, 2012
AASTI AVHRR GAC	IR	4 km swath	Jan-Dec, 2012

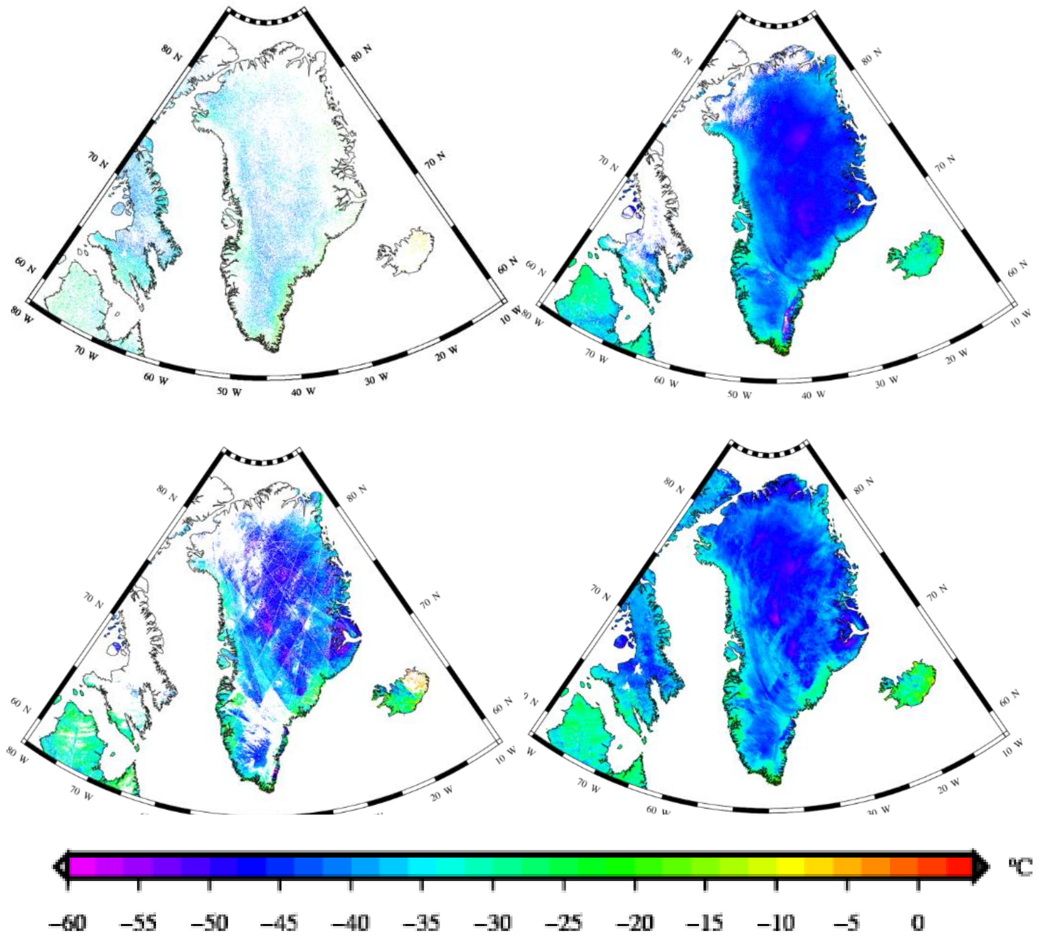

Figure 2-6: Examples of aggregated IST observations from Jan 9th, 2012 over the Greenland Ice Sheet. Top row is Level 3 AASTI GAC (left), Level 3 Modis Aqua and Terra (right) and bottom row is Level 3 AATSR (left) and Level 4 OI based on all three input data sets (right).

In parallel to data production, an LST_cci specific model run was carried out without additional data to use as control against the assimilated version. Six hourly forcing data from the RCM is used to drive the SMB model where surface energy balance variables are used to calculate the ice surface temperature and melt potential. When melt occurs, the model calculates the retention of liquid meltwater and refereezing within the snowpack and deeper firn layers. The sum of precipitation and runoff of meltwater gives the daily surface mass budget over the ice sheet. The SMB model is described in full in Langen et al. (2014, 2018) [RD08, RD-09] and the RCM set up is described in Mottram et al. (2017) [RD-10]. The schematic diagram in Figure 2-2-2 shows how SMB is calculated.

In this study, the quality of the modelled LST in the control run is assessed through a comparison with the LST_cci data. Subsequent runs assimilate the LST_cci in the SMB model via the LST variable. As the LST is calculated at six hourly intervals in the model and daily in the dataset, an interpolation routine is applied to simulate the daily cycle before adding values to the input data set driving the model. To avoid model instabilities, the observed IST is statistically weighted with the modelled IST before calculating the potential production of melt water and temperature in the snowpack. Finally, the daily SMB is calculated and compared with the control run and observations from PROMICE weather stations.

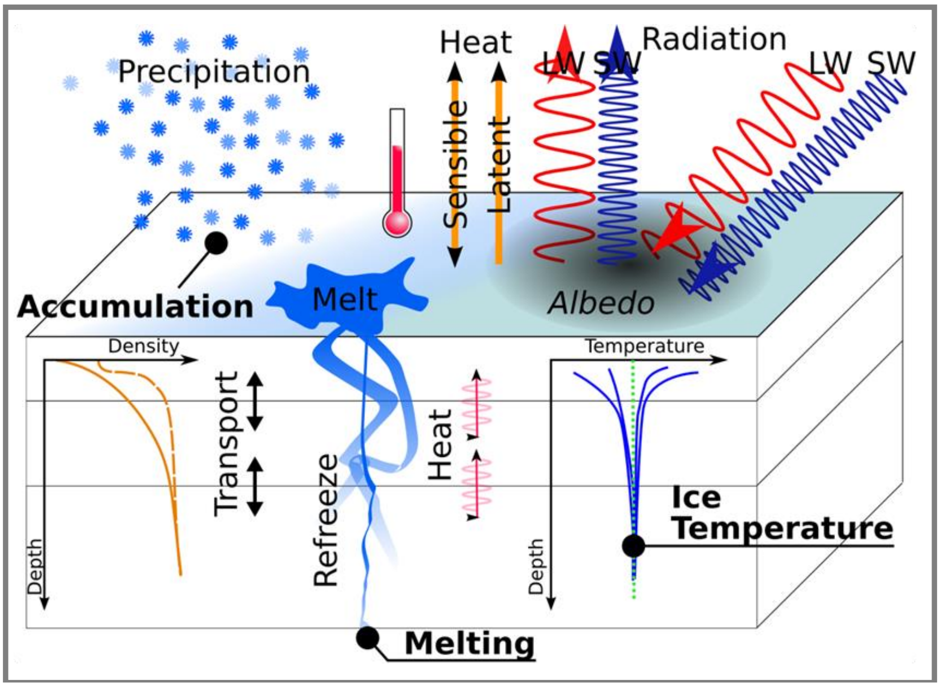

Figure 2-7: Schematic diagram showing the SMB calculation from RCM output. (image credit: Christian Rodehacke, DMI)

2.2.2.3 Results

Model simulation experiments and sensitivity studies are still ongoing (expected through to the end of January 2021), therefore in this report the focus is on the LST_cci data products.

Thermal infrared satellites observe the skin of the snow and ice surface, which can deviate substantially from e.g. a T2m observation [RD-11, RD-12]. For a proper validation of the satellite products, it is therefore important compare against the radiometric surface temperature. These types of observations are available from the Operation IceBridge project [RD-13], which conducted flight campaigns, carrying a thermal infrared radiometer. These observations have been used to determine the quality of the different satellite products both in terms of spatial variability and any offsets. Figure 2-8 shows two examples of MODIS products and AASTI products compared against Icebridge observations.

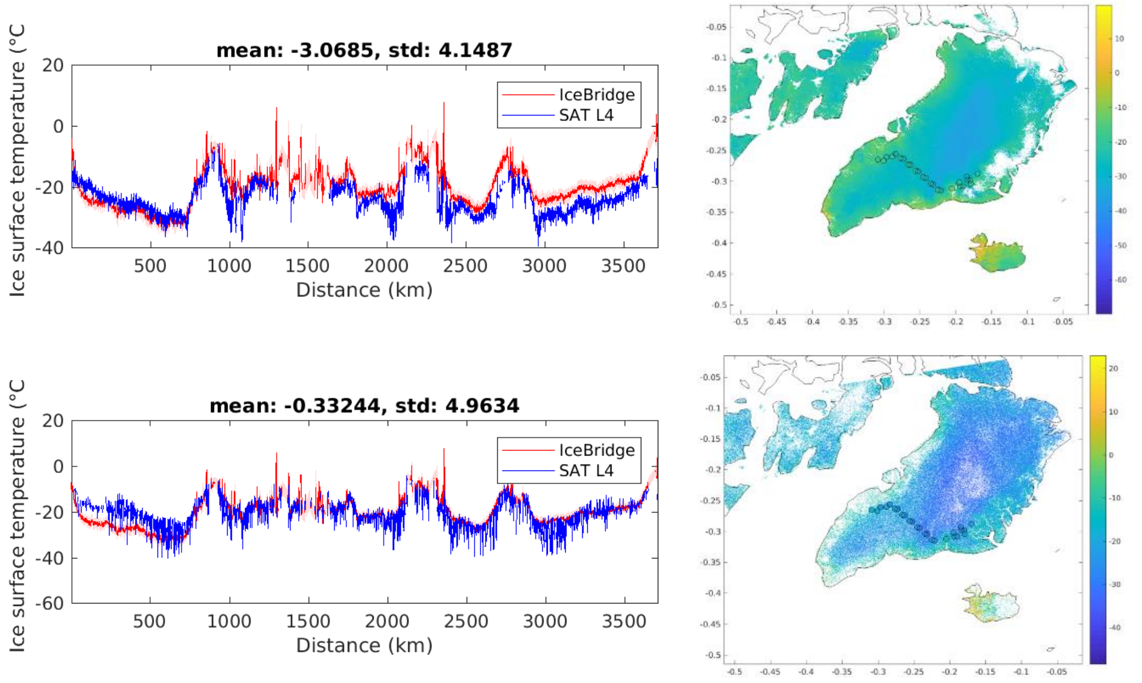

Figure 2-8: Validation of MODIS (top) and AASTI (bottom) level 3 IST products against IceBridge observations from May 8th, 2012. Left figures show along track surface temperature observations and right figures show aggregated satellite IST fields from the day with overlaid IceBridge observations (circles)

The results in Figure 2-8 show that the aggregated MODIS observations are typically cold compared to the IceBridge observations, whereas the agreement is better for the AASTI AVHRR GAC data. It is also clear, however, that the pixel-to-pixel variability in the aggregated MODIS observations is smaller (e.g. lower standard deviation) than in the AASTI observations, probably due to a better coverage. The examples in Figure 2-8 are representative for the other IceBridge comparisons and it was therefore decided to use a dynamical bias correction of the MODIS products against the AASTI GAC data [RD-14] when combining the L3 products into a level 4 product. Daily gap free estimates of the Ice surface temperature for the Greenland Ice Sheet in a 0.01° longitude and 0.02 latitude resolution were generated for the year 2012. The resulting L4 product is shown in Figure 2-9 (right) and a comparison against surface temperature from IceBridge shows that the L4 product performs satisfactorily in terms of quality.

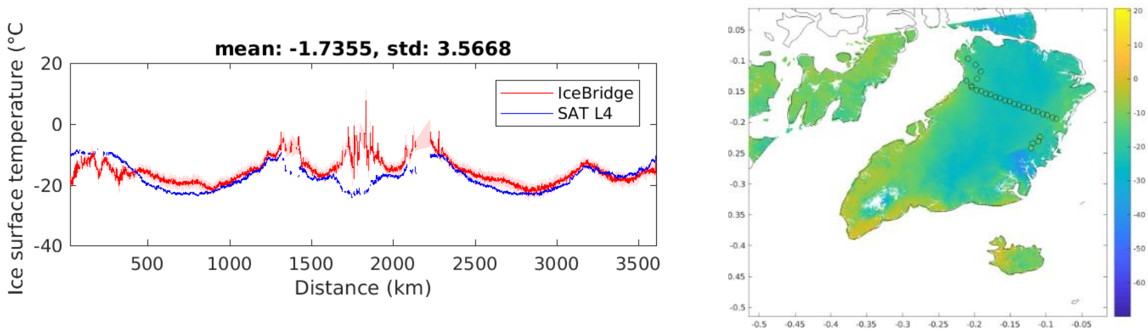

Figure 2-9: Example of Level 4 IST observations compared against IceBridge observations

The daily level 4 fields provide the input for the modelling analysis. Results from the modelling are expected to be ready by the end January 2021 and a journal article highlighting their use is in preparation.

2.2.2.4 Conclusions

LST_cci L2 MODIS Aqua/Terra data have been used together with AVHRR data (sourced elsewhere) to create daily L4 IST data for Greenland. These L4 data will be ingested into an SMB model, which is driven by RCM output, to estimate ice melt and retention. The impact of using observed IST data in the model will be assessed by comparing modelled and observed estimates of these parameters for the extreme melt event of 2012.

Analysis against airborne IST observations suggests that the LST_cci MODIS data may be cold biased by several K. The equivalent AVHRR data agree do not exhibit such a cold bias. However, the variance of the agreement between MODIS and the airborne IST observations is found to be lower than for the equivalent AVHRR data. After implementing a bias-correction to the MODIS data, the agreement between the derived L4 IST data and airborne IST data is found to be satisfactory.

2.2.3 Feedback on scientific utility of the LST_cci products

The LST_cci products was very easy to use in this study. It is appreciated that a special data delivery was set up for this project to deliver Level 2 swath observations. For high latitude regions, it is not feasible to divide products into ascending and descending, but the level 2 data worked very well. The use of the data was very easy due to the same file formatting and naming conventions across the different sensors.

The scientific quality of the products appears to be an area where improvements could be made in the future. The validation showed a general offset of the MODIS products, compared to IceBridge observations, but there were also regions where 30-40 K offset were visible that do not look like typical cloud contamination. Such discrepancies are very large and could be examined in large detail in future algorithm improvements. In general, it is suggested that dedicated IST algorithm improvements could be carried out in order to improve both on the bias and on the large regional errors presented in this study.

2.3 Urban Case Study: A global investigation of Surface Urban Heat Islands (RUB)

2.3.1 Key Messages

- The SUHI intensity estimates derived from the four 0.01° LST_cci custom products are consistent in terms of peak time.
- The SUHII magnitude of the TERRA_MODIS_L3C 0.01° v1.0 data is slightly higher than that of the ERS-2_ATSR_L3C 0.01° v1.0 and ENVISAT_ATSR_L3C 0.01° v1.0 data products.
- The AQUA_MODIS_L3C 0.01° v1.0 data have not been used in this analysis due to problems with cloud contamination.
- The SUHII estimates and hysteretic cycles calculated from the 0.01° LST_cci custom products agree with the published literature.
- The LCC data included in each LST_cci netCDF file need to be updated to reflect LC changes.

2.3.2 Scientific Analysis

2.3.2.1 Aims of the study

The Urban Heat Island (UHI) refers to the relative warmth of urban areas compared to their surrounding rural areas and is the most studied urban climate effect. It is a direct result of urbanization and is driven primarily by the conversion of natural surfaces to impervious surfaces. The intensity of the Surface UHI (SUHII), which is the difference between urban and rural LST, exhibits seasonal hysteretic cycles (i.e. looping patterns), the shape and direction of which vary across climate zones. For instance, in wet climates, SUHII peaks during the summer and is positive throughout the year, while in dry climates it peaks in spring and is negative during summer and autumn [RD-15, RD-16]. These looping patterns are the result of time lags between the energy and water budget of cities and that of rural areas.

The aim of this case study is to investigate the use of the 0.01° LST_cci custom products for estimating SUHI intensities and for characterizing their temporal behaviour. To achieve this objective, this work uses 24 years (1995 - 2018) of daily day- and night-time LST data over the most densely populated regions of the world and calculates the daily (day- and night-time) SUHII of each city. The overall goal is to analyse these estimates with respect to climate, proximity to sea, elevation, and abundance of vegetation.

2.3.2.2 Data and Method

The LST_cci data used in this case study are the ERS-2_ATSR_L3C 0.01° v1.0, ENVISAT_ATSR_L3C 0.01° v1.0, TERRA_MODIS_L3C 0.01° v1.0, and AQUA_MODIS_L3C 0.01° v1.0 IR data products. The sensing time and the data availability of each product are given in Table 2-3, while the regions of interest of the employed data are presented in Figure 2-10. The selected regions (25 in total) include the most populated areas in every continent and major climate zone of the world.

To identify and delineate the cities included in each focus region (Figure 2-10), information from the ESACCI Land Cover (LC) product is used. The ESACCI LC product provides global land cover maps at 300 m and is available from 1992 to 2018. In this work the annual LC data are resampled to the LST_cci 0.01° × 0.01° grid, by calculating the LC class (LCC) fractions of each grid cell. Then, a binary mask of all the pixels that have an urban fraction greater than or equal to 90% is created for every year between 1995 and 2018. These urban masks are filtered to remove any small objects and each cluster of 9 or more connected pixels that remains is given a unique label. To ensure consistency through the years, the same unique label is given to all the instances of each city.

Table 2-3: A summary of the LST_cci products used in the study.

Product String	Sensor type	Resolution	Data availability	Local overpass time
ERS-2_ATSR__L3C 0.01° v1.0	IR	0.01°	August 1995 – June 2003	10:30 am / pm
ENVISAT_ATSR__L3C 0.01° v1.0	IR	0.01°	July 2002 – April 2012	10:00 am / pm
TERRA_MODIS_L3C 0.01° v1.0	IR	0.01°	February 2000 – December 2018	10:30 am / pm
AQUA_MODIS_L3C 0.01° v1.0	IR	0.01°	July 2002 – December 2018	01:30 am / pm

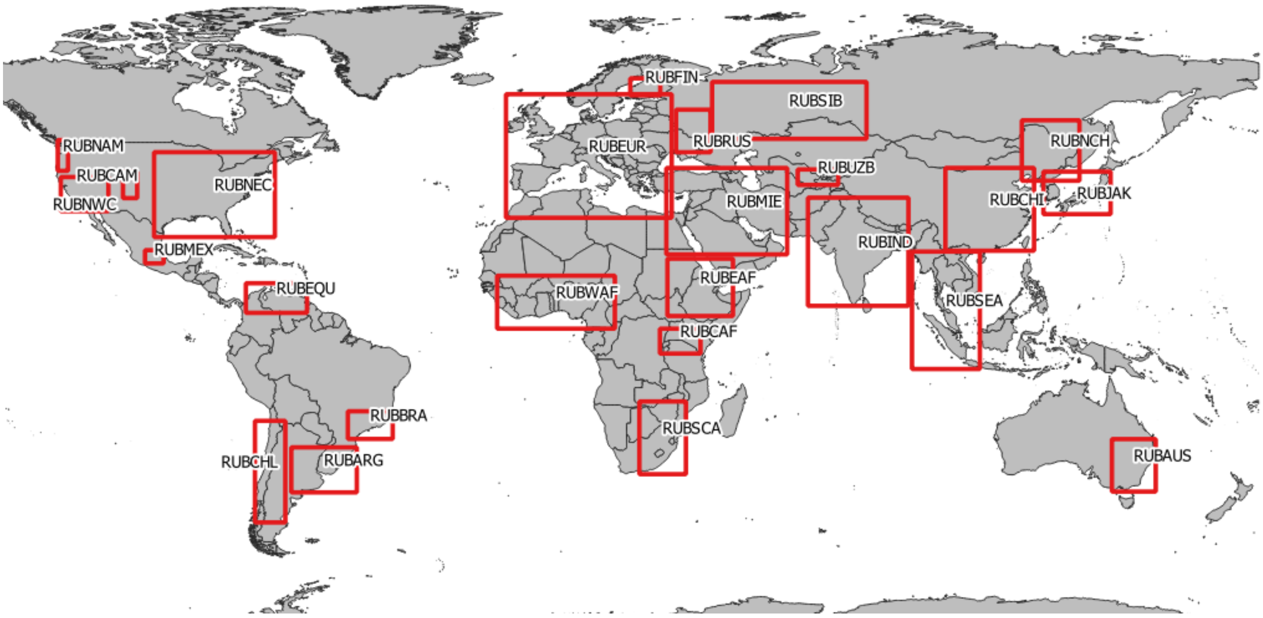

Figure 2-10: The regions of interest for LST data used in RUB's UCS.

For the identified cities, masks that delineate all the natural pixels that are appropriate for calculating the SUHII are also created. This is done using the algorithm proposed in [RD-16], which creates and expands a buffer around each city until its size is approximately that of the urban area. To ensure consistency in the SUHII estimates over the years, a single rural mask, representative for all the years between 1995 and 2018, is created for each city. This is achieved by selecting only the buffer pixels that comply with the following criteria:

- the rural LCC fraction is ≥90% for every year between 1995 and 2018;
- the urban and water LCC fractions are equal to 0% for every year between 1995 and 2018, and
- the pixel elevation does not differ by more than +/- 200 m from the median elevation of the corresponding city.

The urban and rural masks are then used to calculate the urban and rural daily LST means for each city. This is done separately for the day- and night-time LST, and for each LST_cci data product used in this case study (Table 2-3). To ensure the calculation of reliable means, only pixels where the LST value is between 240 K to 350 K and the LST total uncertainty is below or equal to 2 K are used. In addition to these two tests, a Median-Absolute-Deviation outlier test is also used to remove any remaining outliers (the test's statistics are calculated from all the available LST data for each city, product, and year separately). Finally, the daily SUHIIs for each city are calculated as the difference between the daily urban and rural LST means as shown in Equation 2-11. This is done separately for the day- and night-time data and for each one of the four 0.01° LST_cci data products used in this work.

Equation 2-11 $$\boldsymbol{SUHII = \overline{LST}_{urban} - \overline{LST}_{rural}}$$

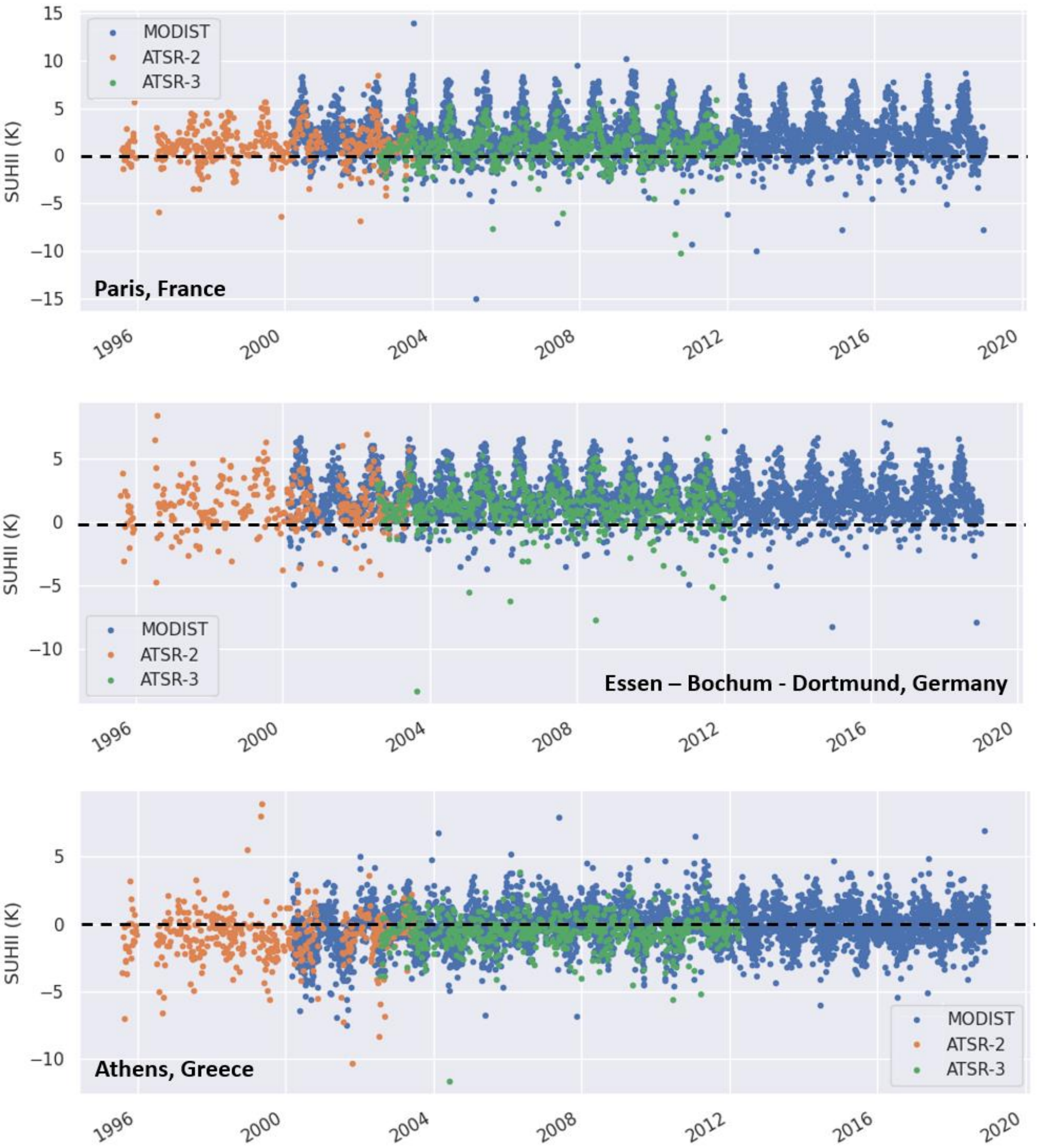

Figure 2-11: The daily SUHII for Paris, France, Essen-Bochum-Dortmund, Germany, and Athens, Greece, for the years 1995 to 2018.

2.3.2.3 Results

Figure 2-11 presents the 1995-2018 daily 10:00/10:30 a.m. SUHII for Paris (France), Essen-Bochum-Dortmund (Germany) and Athens (Greece). Overall, the LST_cci 0.01° custom products provide consistent estimates of SUHII in terms of peak time. The SUHII magnitudes are also similar, but the estimates from the TERRA_MODIS_L3C 0.01° v1.0 data are somewhat warmer than those from the ERS-2_ATSR_L3C 0.01° v1.0 and ENVISAT_ATSR_L3C 0.01° v1.0 data products. This is especially apparent in Paris (Figure 2-11: The daily SUHII for Paris, France, Essen-Bochum-Dortmund, Germany, and Athens, Greece, for the years

1995 to 2018.Figure 2-11), where the maximum daytime SUHII for the years 2000 - 2008 is approximately 7 K for Terra MODIS and 5 K for ENVISAT and ERS. The difference between the MODIS and ENVISAT SUHII estimates is partially attributed to differences in the sensing time of the two instruments, which are not corrected. From Figure 2-11 it also clear that the presence of outliers is limited in the TERRA_MODIS_L3C 0.01° v1.0, ERS-2_ATSR_L3C 0.01° v1.0 and ENVISAT_ATSR_L3C 0.01° v1.0 data products, however, this is not the case for AQUA_MODIS_L3C 0.01° v1.0, where cloud contaminated pixels have been found (not shown).

The SUHII data of Figure 2-11, agree with the published literature [RD-15, RD-16]. In particular, the SUHII of Paris, which is in a wet cool climate, is positive throughout the year, while that of Athens, which is in a dry warm climate, is negative during the summer and positive in winter and spring. These conclusions are corroborated by the SUHII hysteretic curves presented in Figure 2-12 for the Continental (Koppen-Geiger climate zone: Dfb) and Mediterranean (Csa-Csb) regions in Europe. The data of this figure are calculated by aggregating the SUHII estimates from approximately 450 cities for the years 2013-2018 and reveal how the SUHII seasonal variations differ as a function of climate and biome. However, it is important to note that these differences are only evident in the daytime LST data. The night-time SUHII hysteresis curves are similar between the Continental and Mediterranean regions and follow an almost linear increase from winter to summer and a linear decrease from summer to winter (Figure 2-13).

2.3.2.4 Conclusions

This case study is still ongoing, but the preliminary results presented in this report suggest that the 0.01° LST_cci custom products can be used for estimating SUHIIs. In general, the SUHII estimates calculated from the MODIS, ENVISAT and ERS LST products are consistent with each other, but some differences in the SUHII magnitudes may be observed. These differences are more pronounced between MODIS and ENVISAT SUHIIs than between ENVISAT and ERS. (It should be noted that the MODIS and ATSR instruments have differing algorithmic approaches so some differences are expected.) This observation suggests that using unhomogenized multi-sensor 0.01° LST_cci data can be problematic and can thus hamper the use of the multi-sensor LST_cci 0.01° data in long-term SUHII studies. The results of this case study also suggest that the presence of cloud-contaminated pixels is limited, but extra caution is required when working with the AQUA_MODIS_L3C 0.01° v1.0 data product.

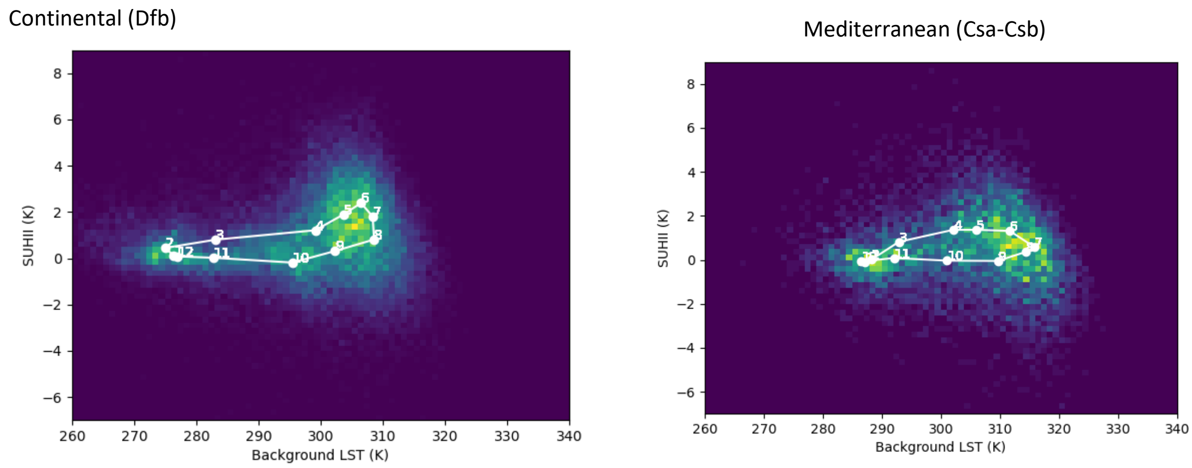

Figure 2-12: The 10:30 SUHII hysteretic curves for the Continental and Mediterranean regions in Europe derived from TERRA_MODIS_L3C 0.01° v1.0 LST_cci data product for the years 2013-2018. The white line in each plot represents the monthly means.

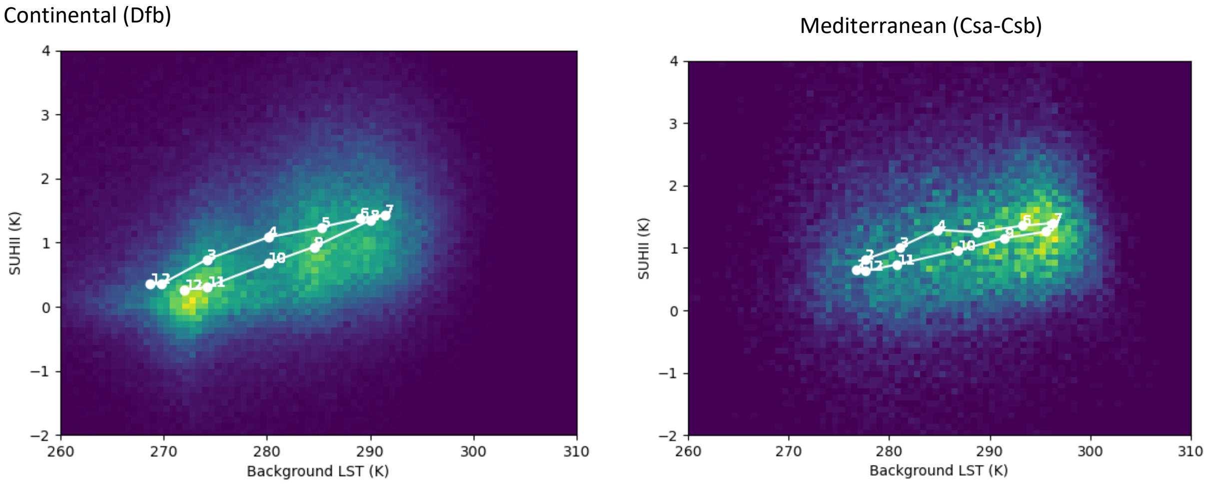

Figure 2-13: The 22:30 SUHII hysteretic curves for the Continental and Mediterranean regions in Europe derived from TERRA_MODIS_L3C 0.01° v1.0 LST_cci data product for the years 2013-2018. The white line in each plot represents the monthly means.

2.3.3 Feedback on scientific utility of the LST_cci products

In general, the LST_cci 0.01° custom products are easy to use and well documented. All the products used in this case study had the same variables and attributes, which facilitated their processing considerably. The main difficulty encountered in processing the LST_cci data was the mosaicking and stacking of the daily data over large areas, such as Europe, which is very memory demanding. Thus, it would be very useful if the data from each orbit were mosaiced beforehand and provided as tiles, similar to the gridded MOD11/MYD11 data products of NASA.

This case study relies heavily on ancillary LC data for identifying and delineating the cities in each LST image. Even though each 0.01° LST_cci netCDF file includes a variable with the LCC label of each pixel, it was found that this information did not change with time. Hence, in future releases, it is suggested the LCC data of each LST_cci netCDF file to change as a function of year.

In SUHI studies, the satellite view zenith angle (SATZE) is important for filtering and interpreting the LST. This is because the LST between east and west building facets can differ considerably within a day. Using the LST_cci data, this information cannot be obtained directly from the SATZE variable, but only after combining it with the satellite azimuth angle (SATAZ). In future releases it is suggested that the SATZE angles are provided as signed floats where the "+" and "-" signs note if the satellite views the east or west side of the surface objects.

Finally, it was found that the latitude and longitude values of the global attributes "geospatial_lat_min", "geospatial_lat_max", "geospatial_lon_min", and "geospatial_lon_max" need to be corrected by half pixel in order to be equal to the actual bounding box coordinates of each LST image. The values currently provided are the latitudes and longitudes of the centre of the four corner pixels.

2.4 The role of LST characteristics in the data-driven simulation of terrestrial carbon fluxes (MPI-BGC)

2.4.1 Key Messages

- AQUA_MODIS_L3C 0.01° v1.0, TERRA_MODIS_L3C 0.01° v1.0, MSG_SEVIRI_L3U as well as NASA MODIS MxD11A1 and a customized LSA SAF SEVIRI LST product are ingested into the data-driven modelling set-up 'Fluxcom'. Their usefulness in the simulation of carbon fluxes is tested in cross-validation experiments at eddy-covariance sites.
- In the prepossing of the LST_cci SEVIRI data, inconsistencies across the temporal record regarding the spatial extent of the fields and the availability of uncertainty information as well as residual cloud contamination were identified. Work on AQUA_MODIS_L3C 0.01° v1.0 & TERRAMODIS_L3C 0.01° v1.0 has not started yet due to open data requests (expected for v2.0 release).
- Depending on the application, temporally/spatially averaged or instantaneous LST values would be desirable.
- The availability of ancillary fields on observation and solar geometries as well as detailed uncertainty information and land cover are appreciated.

2.4.2 Scientific Analysis

2.4.2.1 Aims of the study

LST is one of the most influencial factors on land-atmosphere fluxes of carbon, water, energy, and an important indicator of the state of the vegetation and land surface.

In this user case study, the role of LST in carbon flux simulations is tested in the data-driven set-up 'Fluxcom' [RD-17]. Specifically, the effects of retrieval methods and the added value of hourly (SEVIRI) as opposed to a maximum of four times daily (MODIS) LST information on the accuracy of simulated net and gross terrestrial carbon fluxes are analysed. The consequences of simulating nadir views from oblique views and attempts to make MODIS observations with a variable overpass time comparable in time are also assessed.

2.4.2.2 Data and Method

Land-atmosphere carbon exchange is simulated with the data-driven set-up called 'Fluxcom'. In this approach, machine learning models are trained with in-situ measured net and gross carbon fluxes as target variables as well as with information on the state of the land surface (mostly space-borne) and with meteorological conditions as predictor variables. The trained model is then supplied with data sets of the same predictor variables used in the training to produce diagnostic estimates of the terrestrial carbon fluxes. In this user case study, the focus is on site-level evaluations rather than on spatially explicit estimates. Consequently, factorial cross-validation experiments with different LST data sets as predictors are performed at approximately 300 European flux tower sites, and their accuracy in terms of modelling efficiency and differences compared to observations will be evaluated.

For this, all LST_cci and non LST_cci data streams are referenced to the locations of the eddy covariance (EC) sites for which net and gross carbon flux estimates are available. In the case of the NASA MODIS LST, cutouts of roughly four kilometers around a tower location were obtained from Google Earth Engine, while cutouts of roughly the same size have been requested from U. Leicester for LST_cci MODIS. It needs to be assessed whether the full cutout or a subset of it will be used in the simulations. From the spatially coarser scale MSG_SEVIRI_L3U and LSA SAF SEVIRI, a single satellite pixel whose centre is closest to a tower location is selected in the current processing. This entails a major mismatch between the area of which the in-situ carbon fluxes are representative and the size of the satellite pixel. In the current processing this is accepted and ways to account for spatial heteorogeneity in the machine-learning training will be assessed. Alternative approaches could include the selection of a single SEVIRI pixel in the neighborhood of a tower best representing the conditions at the flux tower site, or the downscaling of SEVIRI LST to higher spatial resolution. Ideas for downscaling SEVIRI LST in the context of this specific application have been developed but deemed too extensive for application given the current limits of time and financial ressources.

Quality checks on the SEVIRI data show that the ancillary information on data quality (uncertainty, number of cloudy pixels) in the LST_cci MSG_SEVIRI_L3U and in the LSA SAF customized SEVIRI product is insufficient to remove unusual sudden decreases of LST of several K. This residual cloud and fog contamination manifests most prominently during nighttime and early morning. As a result, the ancillary data layers are not used, but an outlier detection algorithm was developed. The approach is a modified version after Papale et al. (2006) [RD-18] and consists in checking distributions of the directed differences of consecutive LST values for unusually strong deviations. As the dynamics of LST vary with the time of the day and the season, the distributions are grouped in temporal windows of several days and separately for night, morning, noon and afternoon.

For the NASA MODIS data the data layer on LST uncertainty is used to filter out potentially low quality data. As the data request for AQUA_MODIS_L3C 0.01° v1.0 and TERRA_MODIS_L3C 0.01° v1.0 cutouts is currently open, no information on their treatment can be given.

Estimates of LST as if seen from nadir view are produced following Ermida et al. (2018) [RD-19] for LST_cci MSG_SEVIRI_L3U and NASA MODIS MxD1A1. These geometrical corrections are already included in the customized LSA SAF SEVIRI product. The effects of estimated constant viewing eometry from nadir cannot be estimated for LST_cci MODIS due to averaging across several swaths in the product. For certain applications like this one, additional data layers containing non averaged LST values would be desirable.

As the dynamics of LST in a day are strong, particularly during the MODIS/TERRA morning and MODIS/AQUA noon observations, the variable observation times of consecutive MODIS observations might introduce uncertainties and artifacts in the modelling of the carbon fluxes. Therefore, an attempt is made to scale the NASA MODIS observations to have them comparable in time (not for the noon overpasses). However, this scaling could introduce additional uncertainties that might be larger than in the uncorrected LST values. Thus, the effect of this observation time correction needs to be assessed. Again for reasons of the temporal averaging across multiple swaths, no corrections are applied to TERRA_MODIS_L3C 0.01° v1.0 and AQUA_MODIS_L3C 0.01° v1.0.

The NASA MODIS LST data are averaged over all subpixels from the cutout to obtain one time series per EC site. Subsequent gap-filling of all data streams would be beneficial, but is not implemented currently.

2.4.2.3 Results

No cross-validation experiments have been conducted yet because the set-up of the testing environment is work in progress and because data requests for the LST_cci MODIS cutouts from U. Leicester as well as an updated version of LST_cci MSG_SEVIRI_L3U are currently still open.

Work to date has focused on the investigation and assessment of the LST data sets that are currently available for the study. Figure 2-14 shows an example of the filter for residual cloud contamination in the LST_cci SEVIRI LST, where significant cloud contamination is evident.

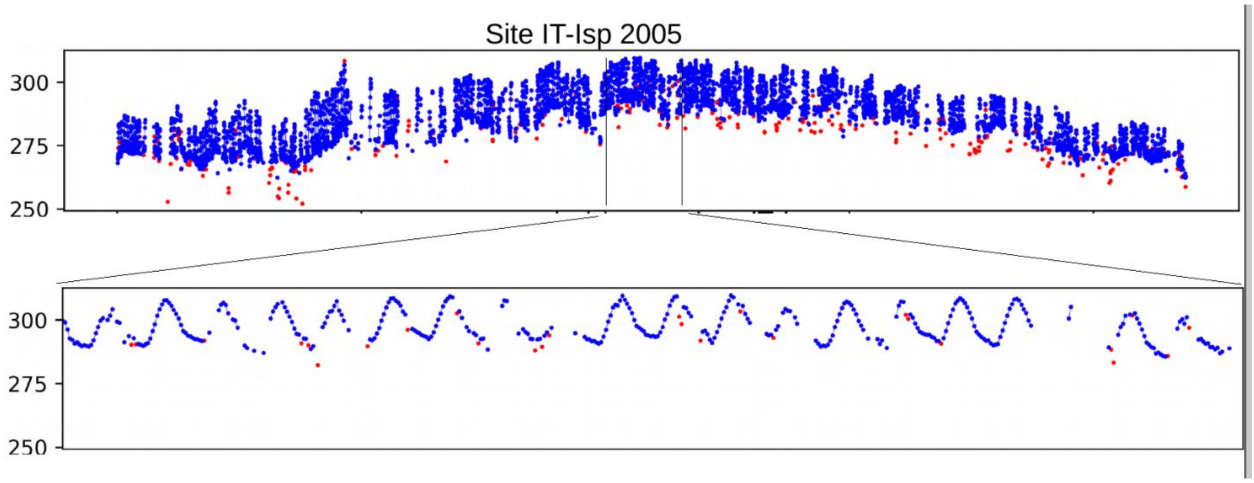

Figure 2-14: Example of the filter for residual cloud contamination in SEVIRI LST at a site in northern Italy for the year 2005. Data points in red are removed by the filter.

Experiments have also been conducted to implement and assess corrections for viewing geometry and overpass time using MODIS Terra data from NASA (Figure 2-15). The magnitude of these corrections can amount to several K and may introduce large uncertainties into the LST data used in the carbon flux estimates.

2.4.2.4 Conclusions

LST data from LST_cci, NASA and the LSA SAF have been obtained for this study, which assesses the role of LST in data-driven simulations of terrestrial carbon fluxes. Initial investigation and analysis of these products has begun, which show that i) there is significant cloud contamination in the LST_cci SEVIRI data and ii) the averaging of multiple MODIS overpasses in the LST_cci data is problematic for this study (further details are provided below).

A scheme to remove cloud contamination in the LST_cci SEVIRI data has been implemented with some success. A geometric correction for LST_cci SEVIRI and NASA MODIS LST data has been implemented, in order to correct the LST observations to nadir (or another selected view angle). A temporal correction for NASA MODIS LST data has also been developed to correct the LSTs to a fixed local observation time, or dynamic observation time with a more consistent insolation. The implications of these corrections for the carbon flux estimates will be assessed during the next phase of the study, which will test the effects of the different LST data sets in estimating carbon fluxes using a machine learning approach.

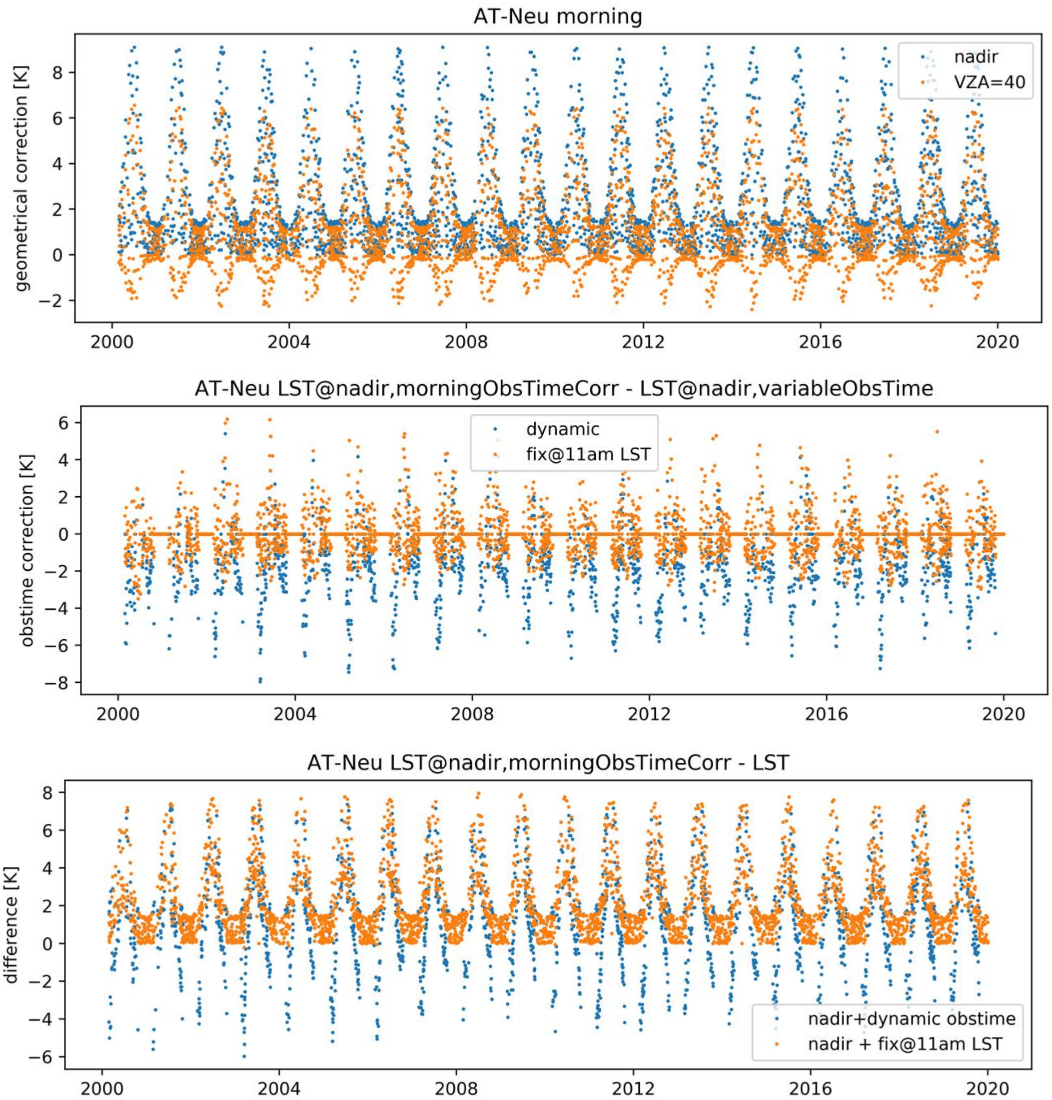

Figure 2-15: Example of the corrections for LSTs derived from the geometric correction from observed view angle to nadir and a view angle of 40° (top), correction to a fixed overpass time of 11 am and variable overpass time with more consistent insolation (middle) and the combined effects of both corrections (bottom).

2.4.3 Feedback on scientific utility of the LST_cci products

Practical experience is mostly limited to the LST_cci MSG_SEVIRI_L3U available for the years 2008-2010 so far. Working with these data was mostly straightforward and the meaning of the variables is clear. The availability of viewing and solar geometries in the files is highly appreciated. Issues that have been noticed or apects that from our user side are recommended are:

- Uncertainty information is only available starting from mid 2008 onwards, and the first period of available data in the record on uncertainty give negative values.
- The spatial extent of the SEVIRI disk changes at some point in the record, so only in the later part also northeastern Europe and parts of south America have valid data.

- The fields 'ncld' and 'variance' are included in the files but have no meaning as the values are instantaneous and nearest neighbour gridding was performed (personal communication with Sofia Ermida). As the LST_cci files have a standardized format across all products, a comment in the file attributes is suggested.
- Residual cloud contamination is detected.
- Requirements for LST characteristics vary between applications, therefore the following is suggested:
    - Provide the full SEVIRI record instead of limiting the available data to 2008-2010. Personal communication with Sofia Ermida revealed that a reprocessing with updated and extended data is planned soon.
    - Include a geometrical correction factor for nadir view in the files (although it is acknowledged that the desirable reference angle might differ between applications).
    - High temporal and high spatial resolution at the same time is highly desirable. Downscaled geostationary LST would be of use for many applications.
    - Also depending on the application, instantaneous or temporally averaged LST might be preferable in terms of data availability, resolution and noise. Therefore, hourly averaged LST is suggested as an additional data layer.

The availability of a high resolution global product in AQUA_MODIS_L3C 0.01°v1.0 and TERRA_MODIS_L3C 0.01° v1.0 is very beneficial. Although work on them has not yet started, from the known processing steps in the products, the following recommendations are given:

- Averaging over all swathes during a day as is done currently is beneficial in terms of data availability and noise. However, it impedes processing steps such as geometrical corrections and a precise temporal allocation eg to ground data. The recommendation from a user prespective is therefore to provide *in addition (not exclusively)* instantaneous LST (despite the fact that also the number of ancillary fields on observation time and angles and uncertainties will be multiplied). Those instantaneous LST observations could/ should represent
    - the observation closest to the nominal overpass time
    - the best quality observation in a day
    - (an averaged LST with restricted range of overpass times closer to the nominal overpass time)
    - All or one of them might include a geometrical correction factor to nadir.

Independently of the product, gapfree LST data would be useful for several applications (including this one). However, requirements for strictness of quality control and therefore also gap structure will vary between applications, which might render this activity impossible.

2.5 Analysis of Urban Surface Temperatures in Romania (MeteoRomania)

2.5.1 Key Messages

- LST and T2m are compared in urban areas and to explore the Urban Heat Island Intensity (UHII) at a country scale.
- The results show that LST and T2m are very well correlated in urban areas (r~0.9), particularly during the day.

- The surface UHII (SUHII), which is calculated from LST data, is influenced by local geography and varies spatially within the urban area.
- The MODIS/Aqua and MODIS/Terra LST_cci products are straightforward to use in urban climate research, but control quality related to cloud contamination is recommended.

2.5.2 Scientific Analysis

2.5.2.1 Aims of the study

The study aims at exploring the potential of the MODIS LST_cci products for performing (1) an inter-comparison between the LST and T2m in urban areas, and (2) exploring the Surface Urban Heat Island Intensity (SUHII) at country level, i.e. Romania.

2.5.2.2 Data and Method

The LST_cci products used in this study are customised TERRA_MODIS_L3C and AQUA_MODIS_L3C daily day/night 0.01° latitude/longitude data over Romania. The LST was extracted from both MODIS LST_cci data sets for 77 urban areas from Romania (> 30,000 inhabitants), for the period 2000-2018. In order to ensure a homogeneous data representation, only images with at least 50% data coverage for each city were selected. Extreme Outliers in the LST_cci data occur quite frequently, presumably due to cloud contamination, and these were removed and excluded from the analysis (see Section 2.5.3).

The comparison between LST and T2m was performed for 6 cities of comparable size located in different geographic conditions, using the LST values of the pixel overlapping the WMO (World Meteorological Organisation) meteorological stations which monitor the local climate of each city.

The SUHII of each city with more than 30,000 inhabitants was computed both for daytime and night-time, as the difference between (1) the average LST of the urban pixels from the built-up administrative perimeter of each city, and (2) the average LST of the non-urban pixels from the surrounding rural buffer of each city. Water and wetland areas were also excluded from the analysis.

The urban and rural areas were identified using the land cover information retrived from CORINE Land Cover (https://land.copernicus.eu/pan-european/corine-land-cover).

2.5.2.3 Results

The results indicate very good correlations between LST and T2m for all the locations analysed both for daytime and nighttime. For example, at the peri-urban weather station București-Băneasa, which monitors the climate of Bucharest, the Pearson correlation coefficient is between 0.817 and 0.951 (Figure 2-16). The lowest correlations are returned for summer, when the heterogeneity of the radiative budget may vary significantly over small areas due to influencing factors, such as albedo, latent heat flux, or cloudiness.

Figure 2-17 and Figure 2-18 provide an overall view of the SUHII at country scale in July, which is generally the warmest month of the year Romania. The SUHII data shown here are derived from an arithmetic mean of both MODIS/Terra and MODIS/Aqua data. For daytime, the lowest values can be observed in the southern areas due to either intense regional heating which as a result of two factors: (1) the regional extent and intensity of the warming dominates over the urban influence on the LST, and (2) the proximity of the Black Sea coast has a very strong influence on the urban climate in the SE areas. The highest SUHIIs occur in the North-Western part of the country, where the contrast between the built-up areas and regional background (i.e. very often the coldest area in Romania) enhances the SUHI formation and strengthening.

The T2m Urban Heat Island (UHI) is generally correlated with the size of the city [RD-20]. At country level, the SUHII is quite well correlated with urban surface area and population during the nighttime (i.e. Pearson correlation coefficients 0.443, and respectively 0.372), while the daytime correlation is significantly lower (Figure 2-19).

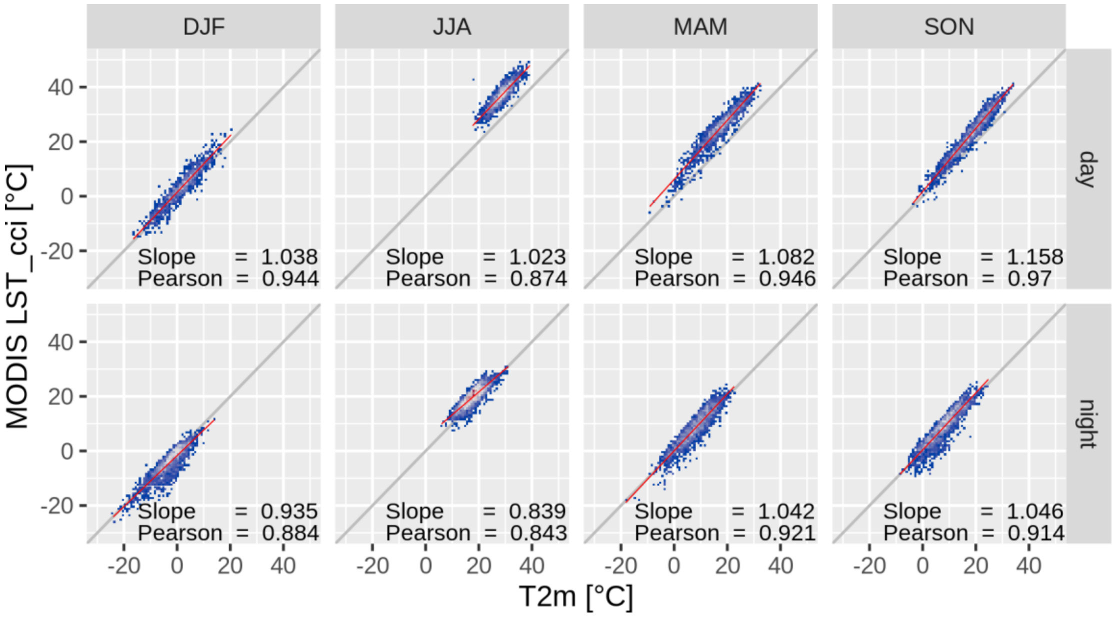

Figure 2-16: Comparison between MODIS LST_cci and T2m at București-Băneasa weather station

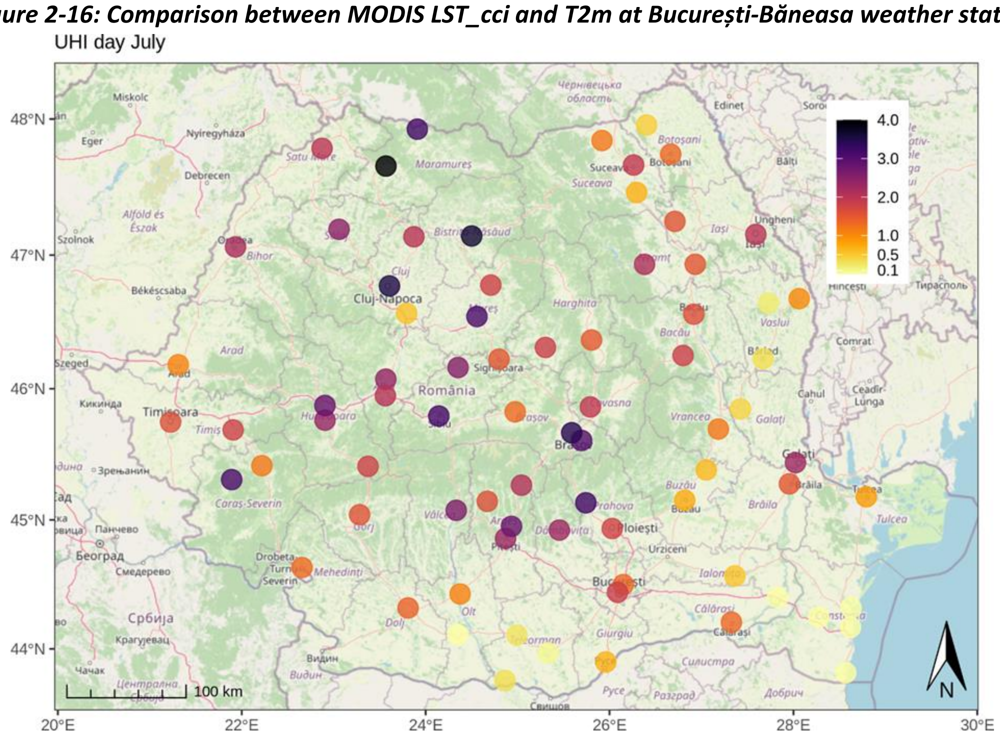

Figure 2-17: July daytime SUHII (°C) of the urban settlements with more than 30,000 inhabitants over Romania

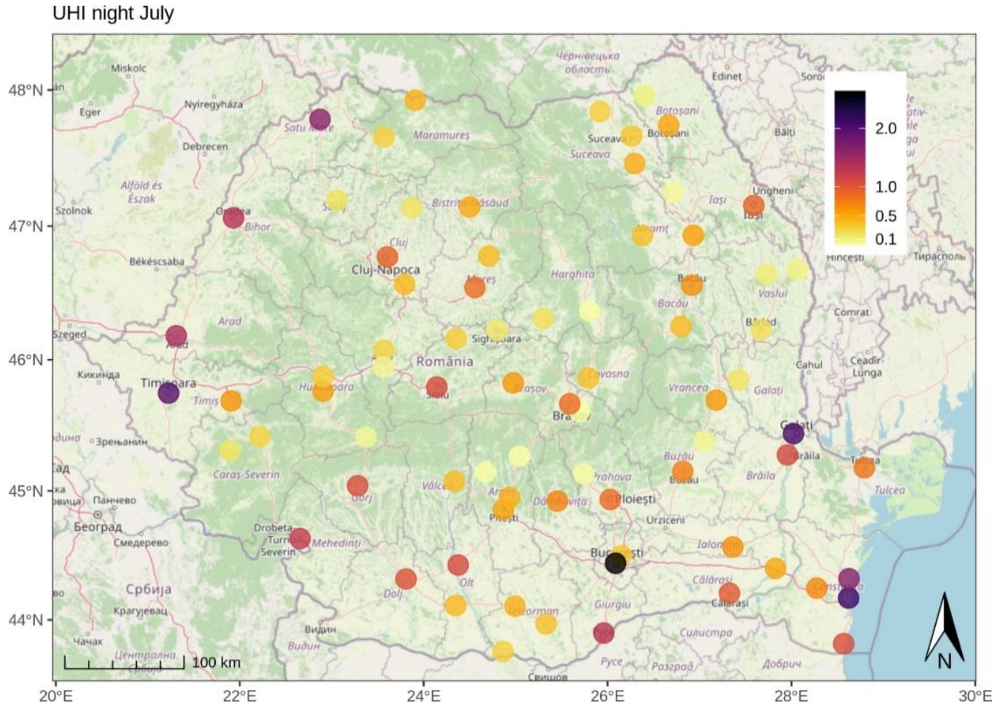

Figure 2-18: July nighttime SUHII (°C) of the urban settlements with more than 30,000 inhabitants over Romania

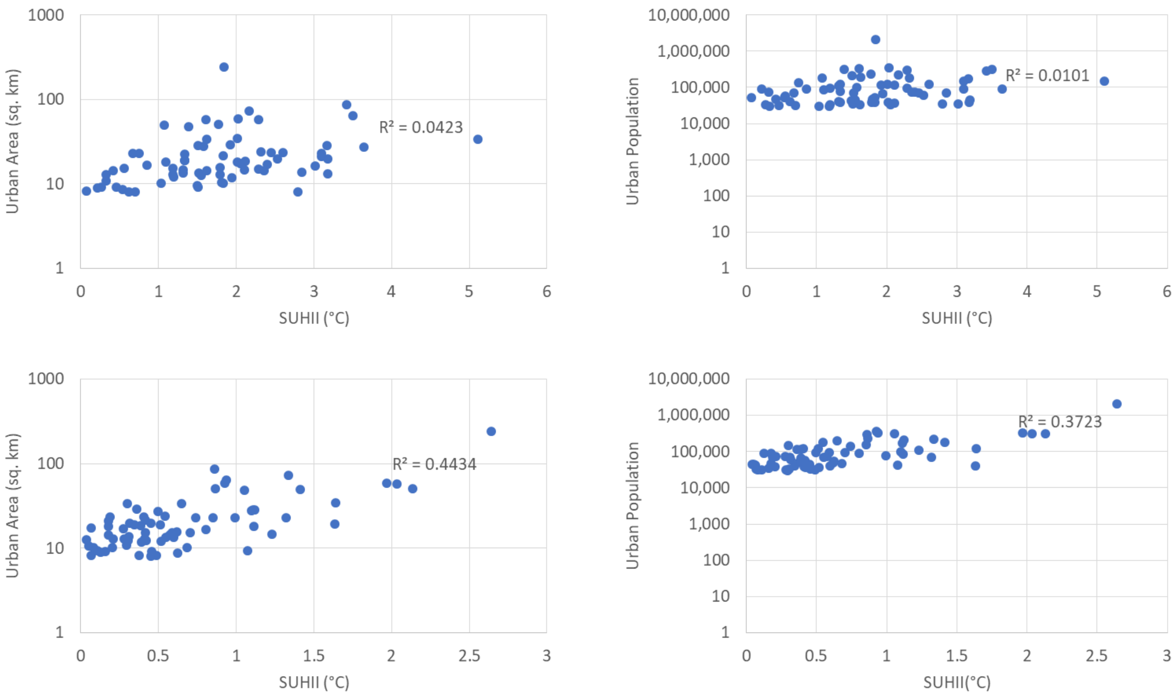

Figure 2-19: Scatterplot of average SUHII (°C) vs urban surface area and population in Romania (daytime – upper row, and nighttime – lower row)

2.5.2.4 Conclusions

Based on analysis of the LST_cci MODIS 0.01° products, this study demonstrates that LST and T2m are very well correlated over urban areas, especially considering the inherent differences related to the observations and temporal and spatial mis-match are considered (e.g. satellite areal average vs station point observation).

The data suggest that larger cities in Romania have considerable influence on the surface temperature, and the SUHI is clearly outlined both during day- and night-time. However, the regional geography has a strong impact on the SUHII, often dominating over the influence of the built-up areas in Romania, at least in the hottest months. The urban size (i.e. population and surface area) is more important for SUHII amplification during the night.

2.5.3 Feedback on scientific utility of the LST_cci products

The LST_cci products can be used easily in urban climate research, as they provide adequate resolution, hold an excellent accuracy over the area of interest, and address very well the temporal coverage required in climatology.

Some shortcomings include possible outliers identified in the data sets, very likely due to the cloud contamination of images. For example, Figure 2-20 shows low daytime LST values over Romania at the end of June, i.e. below 40^{o}C, leading to a temperature range above 82^{o}C. A summary of such anomalous ranges extracted from the entire LST_cci dataset used in this study is presented for each season in Figure 2-21.

In order to improve the reliability of the results, the data were filtered out using the Rosner method, performed with the rosnerTest() function from the EnvStats R package [RD-21]. Firstly, the LST range was computed for each image as the difference between the percentiles 98 and 2, in order to eliminate the most prominent artefacts. Secondly, the Rosner's generalized extreme Studentized deviate test detected the outliers within the resulted datasets [RD-22, RD-23], and anomalous LST values were identified within 112 images, which were not considered for the analysis.

The study emphasizes that quality control is highly recommended when using the MODIS LST_cci products in urban climate research, and improvements of the product in this respect would be very useful for end-users.

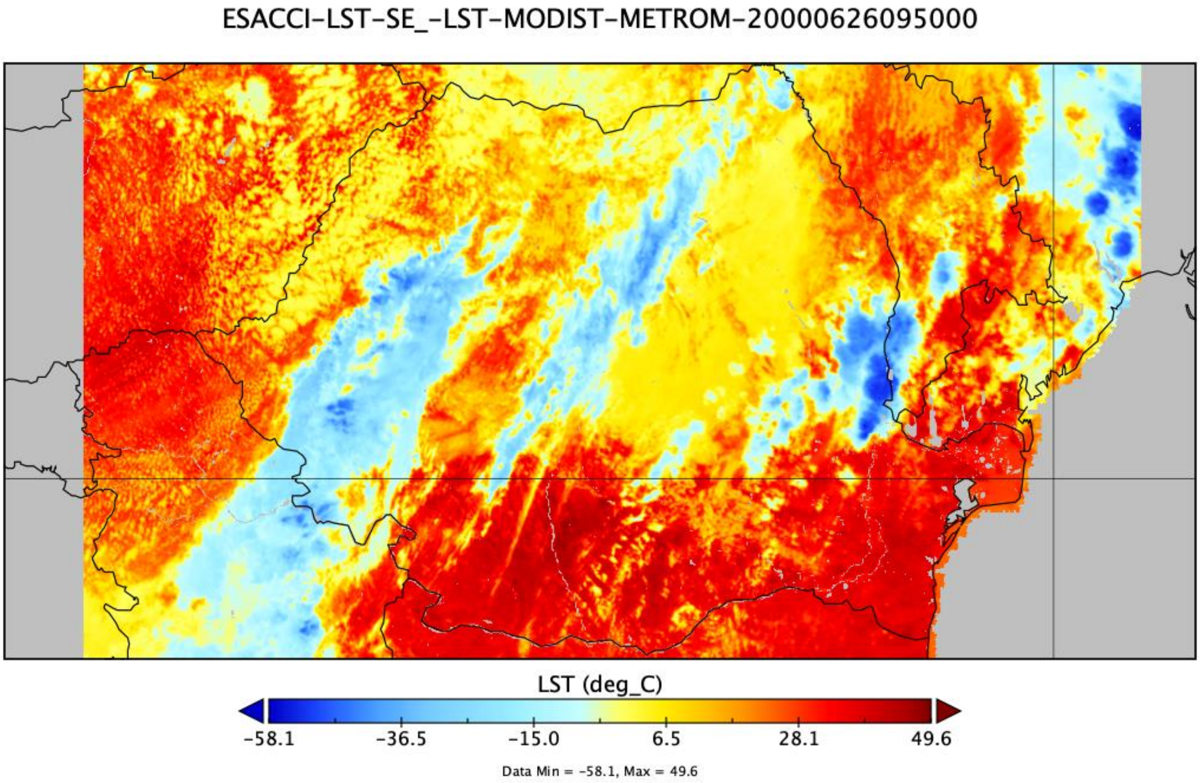

Figure 2-20: Land Surface Temperature over Romania on 26 June, 2000, 09:50 h UTC, extracted from MODIS/Terra

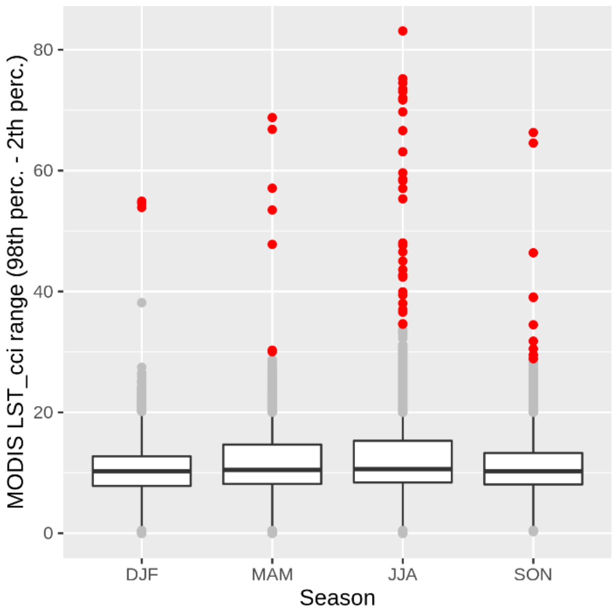

Figure 2-21: Boxplots of the seasonal LST range values. Red dots are the outliers detected with the Rosner test, and not considered in the analysis

2.6 Integration of LST into a Surface Energy Balance Model (LIST)

2.6.1 Key Messages

- Daily LST day- and night-time pan-Australian mosaics are generated using AQUA_MODIS_L3C and Terra_MODIS_L3C 0.01° LST_cci data products
- LST_cci data from two sites in the North Australian Tropical Transect (NATT) will be integrated into a non-parametric Surface Energy Balance (SEB) model (STIC 1.2) for simultaneous estimation of evaporation, transpiration and water stress, and the results will be validated across an aridity gradient and multiple biomes.
- The difference between LST and aerodynamic temperature will be examined within the context of net available energy, fractional vegetation cover and soil moisture class
- An error analysis of the SEB model in the context of partial least square regression to understand the importance of each variable in the model projection will be performed.

2.6.2 Scientific Analysis

2.6.2.1 Aims of the study

LST provides the most important lower boundary condition in surface energy balance (SEB) models and is critical for partitioning evapotranspiration (E) into evaporation (E_E) and transpiration (E_T). The main objective of this study is the integration of the LST_cci data into a non-parametric SEB model called the Surface Temperature Initiated Closure (STIC1.2) to assess the mapping potential of E_E, E_T and water stress (S_T) across the aridity gradient of the North Australian Tropical Transect (NATT), which covers a broad spectrum of environmental and ecohydrological conditions. The model output will be tested and validated at several Eddy Covariance (EC) test sites in Australia.

The first aim of the study was to generate daily pan-Australian mosaics for MODIS Aqua and Terra separated into day and night observations to extract data corresponding to the EC test sites in Australia.

The second aim of this study is the assessment of the spatio-temporal variability of the STIC1.2 model outputs in terms of stability and uncertainty across the EC stations along NATT. The study will examine if there is a systematic trend in STIC1.2 error metrics and if these trends are associated with LST, ecohydrological conditions and land surface heterogeneity.

2.6.2.2 Data and Method

Table 2-4: LST_cci products used for this study case

Product String	Sensor type	Resolution	Data availability	Local time
TERRA_MODIS_L3C 0.01° v1.0	IR	0.01°	Jan 2010 – Dec 2018	10:30 22:30
AQUA_MODIS_L3C 0.01° v1.0	IR	0.01°	Jan 2010 – Dec 2018	01:30 13:30

Mosaics were generated by sorting the datasets according to their filename by sensor, date and time stamp (day/night) separately. Accordingly, the first tile of MODIS Aqua/Terra day- or nighttime in the corresponding folder was defined as reference and all tiles within this folder updated this matrix by replacing NaN values with valid LST_cci data. This results in daily pan-Australian mosaic for MODIS Aqua or Terra day- or nighttime, respectively. Afterwards subsets for the test sites were created. For each site, a block of 3 x 3 pixels surrounding each EC site was extracted and statistical analysis performed (e.g. mean, median, standard deviation); the mean LST is retained and will be used to drive the SEB model.

In the next phase of the study, these 3x3 LST means from the LST_cci products will be integrated in Surface Temperature Initiated Closure model v1.2 (STIC1.2; RD-24, RD-25, RD-26, RD-27). STIC1.2 is independent of any land surface parametrization of the surface and atmospheric conductances. STIC1.2 estimates a water-stress factor by integration of LST into an analytical formulation having a functional dependence of evaporation on moisture availability. Simultaneously STIC1.2 constrains the biophysical conductances through the water-stress factor and environmental variables for estimating the SEB fluxes.

The following metrics will be assessed at each EC site once the LST_cci data have been integrated into STIC1.2, using observations acquired at each EC site:

Equation 2-12: $$\boldsymbol{Residuals_{STIC} = E_{STIC1.2} - E_{observed}}$$

Equation 2-13: $$\boldsymbol{Difference_{LST\_cci} = LST_{cci} - LST_{observed}}$$

$E_{observed}$ and $LST_{observed}$ are the observed evapotranspiration and LST, respectively, at the EC sites. For estimating $\text{LST}_{observed}$, the upwelling and downwelling thermal longwave radiation observations available in the EC tower sites were inverted (http://www.ozflux.org.au/monitoringsites/). The surface emissivity used to estimate $\text{LST}_{observed}$ is based on the fractional vegetation cover.

2.6.2.3 Results

Daily pan-Australian mosaics for MODIS-Aqua and Terra day- and night-time were generated for January 2010 – December 2018 in Matlab using around 114000 single LST_cci tiles.

Subsets of 3x3 pixels for the EC stations Alice Springs Mulga (lat: -22.2828, lon: 133.2493) and Dry River (lat: -15.2588, lon: 132.3706) were extracted for the period 2010-2018 along the NATT. The EC stations in the more humid regions (Howard Springs, Daly River Uncleared) suffered from low data availability in the LST_cci dataset (e.g. due to cloud cover) and were therefore not analysed further.

At the time of writing, LST_cci have not yet been integrated into the SEB STIC1.2 model. However, examples of instantaneous E (in terms of latent heat flux, λE) and sensible heat flux (H) for one arid and one semi-arid site using MODIS Terra data from NASA are shown below. It is hoped that by using LST_cci data in the STIC1.2 model in place of the NASA data, improved results will be obtained during the next phase of this study.

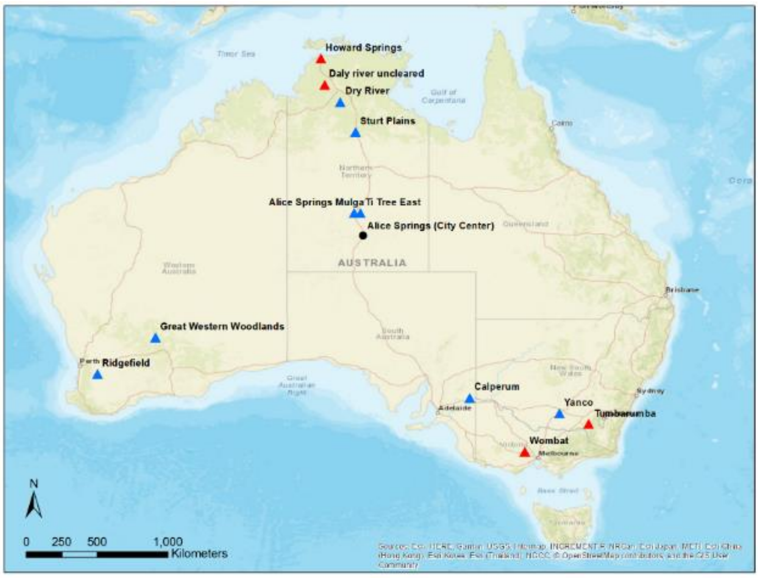

Figure 2-22: Overview of the potential EC (Eddy Covariance) test sites in Australia that are used in the study. For the blue marked stations MODIS Aqua/Terra data are available, while for the red marked stations very few LST_cci data are available (e.g. due to cloud cover) so these stations have been excluded from the study.

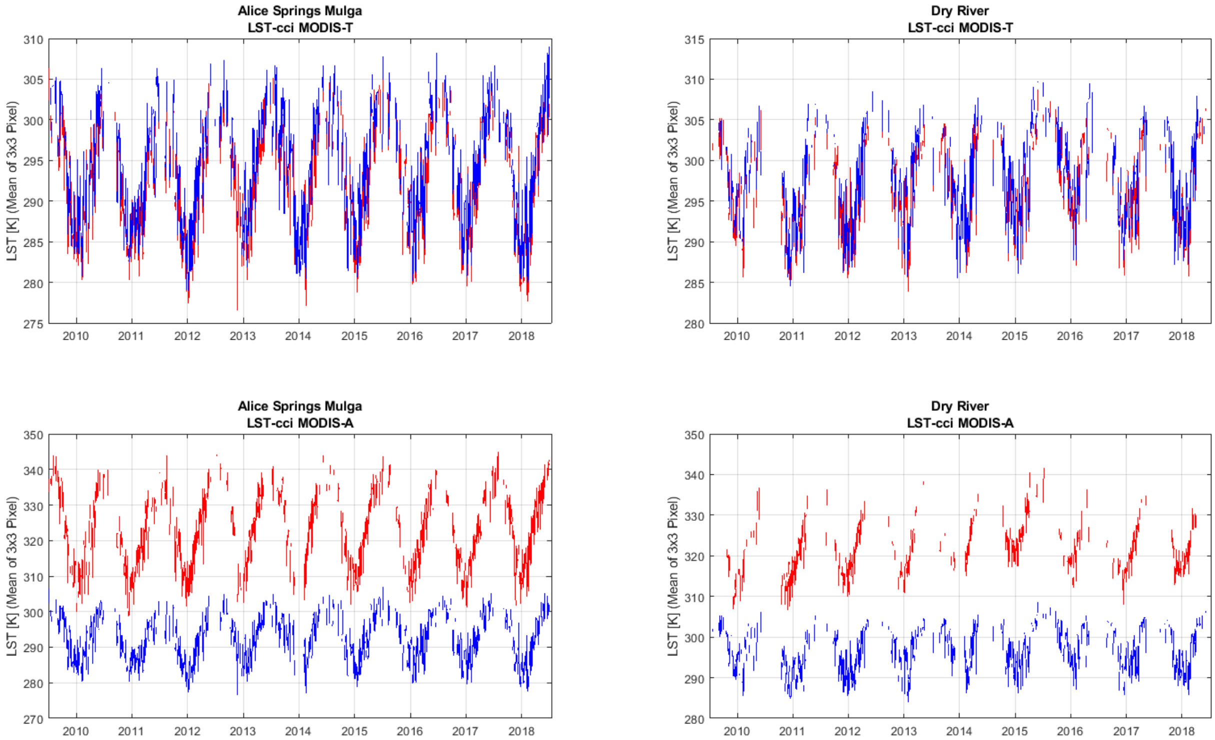

Figure 2-23: Comparison of the LST_cci estimations at two sites in the NATT: Alice Springs Mulga and Dry River. Red lines are the daytime LST observations, blue line represent the night-time observations. MODIS-Terra (top row), which has a morning overpass, has more data than MODIS-Aqua (bottom row), which has an afternoon overpass at 13:30 local time. In general, fewer MODIS data seem to be available at Dry River, which is at the north end of the NATT with humid climatic conditions, compared with Alice Springs, which has a drier climate.

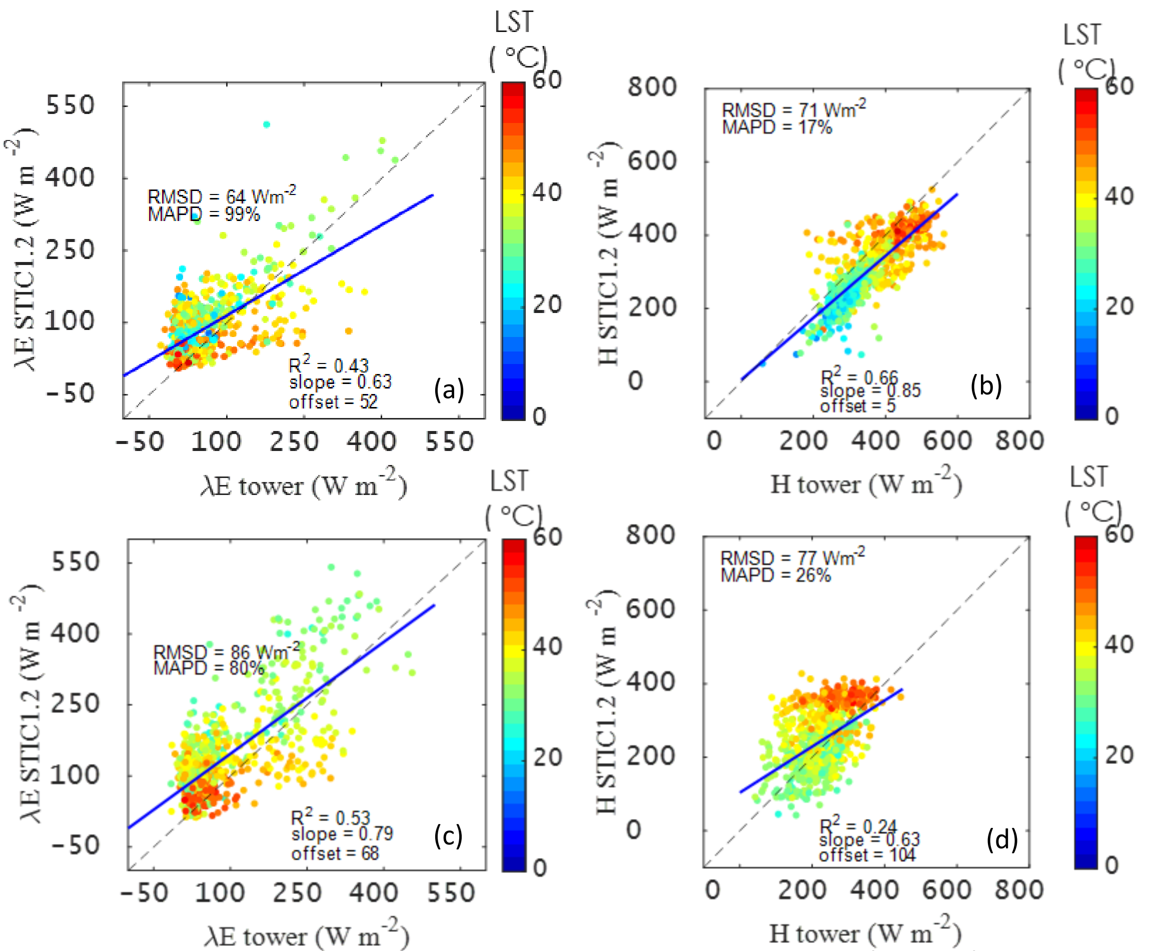

Figure 2-24: An example of evaluation of modelled latent and sensible heat fluxes (LE and H) for different classes of LST in one arid and one semi-arid ecosystem in the North Australian Tropical Transect (NATT) using data from MODIS Terra provided by NASA.

2.6.2.4 Conclusions

Tiled LST_cci data for MODIS Aqua and Terra at 0.01° latitude/longitude have been used to produce pan-Australian day- and night-time LST data sets for the period January 2010 – December 2018. Data corresponding to several EC sites along the NATT have been extracted. Several of the sites suffer from frequent missing data, which is assumed to be due to cloud (expected for very humid sites with frequent cloud cover); these sites have too few data to be of use in this study so are not considered further.

The next step in the study is to integrate the daily time series of LST_cci data into the non-parametric SEB model, STIC1.2, to estimate evaporation, transpiration and water stress. The model output will be assessed and validated using observations from the EC sites. In addition, the LST_cci data will be compared to LSTs observed at the site for additional validation.

2.6.3 Feedback on scientific utility of the LST_cci products

The quality of the LST_cci product is not yet evaluated as the mosaicking of the LST_cci data was an unexpected step that was required during the processing. Naming the LST_cci tiles with a geo-location would be helpful or providing with a clear identification according to the MODIS tiling system or for example the Sentinel-2 tile grid (UTM system). This would make the identification of tiles containing the

LST_cci data of the areas of interest easier. For example, the FLUXNET stations “Alice Springs Mulga” and “Ti Tree East” are both located in the Sentinel-2 tile 53KLR. With this identification code in the filename it would be easy to directly point to the areas of interest.

The netCDF LST_cci products itself was well structured and easy to process them in Matlab.

3. Other User Case Study Reports

3.1 Demonstrate the potential of using a new metric: LST minus air temperature, to evaluate vegetation moisture stress in CMIP6 models (Debbie Hemming & Rob King, MOHC)

3.1.1 Key Messages

- Preliminary analyses have examined seasonal mean LST minus near-surface air temperature differences (LST-T2m) using data from UKESM1 (UK Earth System Model 1) and focusing on areas of grass and crop vegetation with either a C3 or C4 photosynthetic pathway. Two large regions, North America and China, have been examined.
- Differences in physiology between C3 and C4 vegetation means that C4 generally transpire less and show more tolerance to higher temperatures and lower soil moistures compared to C3. With lower transpiration rates, lower surface cooling is expected for C4 vegetation, and it is therefore proposed that areas dominated by C4 vegetation should show a larger mean LST-T2m and larger seasonal change relative to areas dominated by C3 vegetation.
- Results for North America and China show consistently larger differences and seasonal variations in LST-T2m for areas dominated by C4 (grass and crop) vegetation, compared with those dominated by similar C3 vegetation.
- Further initial work (not presented here) to study LST-T2m using LST_cci and ERA5 near-surface temperature has begun in preparation for the evaluation of CMIP6 models.
- Initial work to implement a diagnostic using LST_cci into ESMValTool highlighted a minor issue with the coordinate metadata in the AQUA_MODIS_L3C V1.0 product which showed two latitude coordinates (rather than latitude and longitude) in the 'standard name'. This has now been corrected for further updates of the data (see section 2.1.3).

3.1.2 Scientific Analysis

3.1.2.1 Aims of the study

Land Surface Temperature (LST) provides information on the partitioning and exchanges of energy and water between the land surface and atmosphere. It also influences the timing and productivity of terrestrial vegetation through availability of energy for photosynthesis and evapotranspiration, which exerts a key limitation on vegetation moisture availability. This study aims to assess the potential for a new vegetation stress metric, namely LST minus air temperature (LST-T2m) that can be used for evaluation of large-scale vegetation moisture stress in Earth System Models (ESMs).

Initial analyses for the CMUG and presented here utilise as a first step LST and near surface air temperature from UKESM1 to analyse spatial and temporal variations in LST-T2m for two major biomes (C3 and C4 grass and crop types) across two large regions, North America and China. Physiological differences between C3 and C4 vegetation at the leaf level are expected to show as larger LST-T2m differences across large-scale C4 dominated areas [RD-28].

The results presented here use the land cover from UKESM1 but this work will progress to use biomes characterised using LC_cci Land Cover data, and further work will utilise Soil Moisture data from SM_cci to understand relationships between LST-T2m and moisture stress. The work will address two key science questions: i) Can the LST-T2m metric be used to monitor global-scale vegetation moisture stress across different biomes and regions? and ii) How well do CMIP6 ESMs capture spatio-temporal trends in LST-T2m?

3.1.2.2 Method

LST-T2m differences were examined using output from historical runs of UKESM1 exploiting the monthly mean output stream. For the two areas of interest, North America and China, the ensemble average plant functional type was used to create a seasonal land cover mask for the years 2003-2014. Grid boxes were classified as either C3 or C4 grasses and crops if they covered at least 50% of the grid box area. Seasonal mean LST-T2m values were produced for each of the C3 or C4 masked regions.

3.1.2.3 Results

Preliminary results show clear differences in the LST-T2m differences of C3 and C4 vegetation (Figure 3-1; note the results presented are for modelled data not the LST_cci products). For two large-scale regions, China and North America, areas dominated by C4 vegetation show consistently larger seasonal mean LST-T2m differences compared to C3 dominated areas. The seasonal cycle of LST-T2m for C4 vegetation is also up to 3 times larger across China and about two times larger across North America than for C3 vegetation.

These initial results are consistent with expectations based on physiological differences between C3 and C4 vegetation that lead to generally warmer leaf surface temperature of C4 vegetation, due to lower transpiration rates, compared with C3 vegetation. This difference is accentuated during warmer, drier periods as shown by the larger difference between C3 and C4 dominated areas during summer in both regions.

The results indicate that the LST-T2m metric is able to identify large scale spatio-temporal variations in moisture status of dominant vegetation. This is encouraging for the main work on this study which is scheduled between November 2020 and September 2021 for CMUG WP4.8 and WP4.9.

3.1.2.4 Conclusions

Physiological differences between C3 and C4 vegetation result in consistently higher leaf temperatures for C4 vegetation. Preliminary results show that these differences are clearly evident in the seasonal LST-T2m difference across two large regions, China and North America.

Further work for this study will assess the potential for the LST-T2m difference to be used as a large-scale evaluation metric for vegetation moisture stress responses in ESMs by using the LST_cci as an observation truth to evaluate against.

3.1.3 Feedback on scientific utility of the LST_cci products

Initial work with monthly mean AQUA_MODIS_L3C V1.0 LST_cci products has shown that the data are easy to download and manipulate for inclusion in ESMValTool. This will allow the work to evaluate UKESM1 and other CMIP6 models using the above described methods with the LST_cci product. A minor issue with the header information of the AQUA product was noted, where the 'standard_name' included two latitude coordinates, rather than latitude and longitude. This was important to correct for converting the MODIS_L3C products to a format suitable for inclusion into ESMValTool. After discussions between the LST_cci science team and CRG, the standard name was corrected for the next update of the relevant LST_cci products.

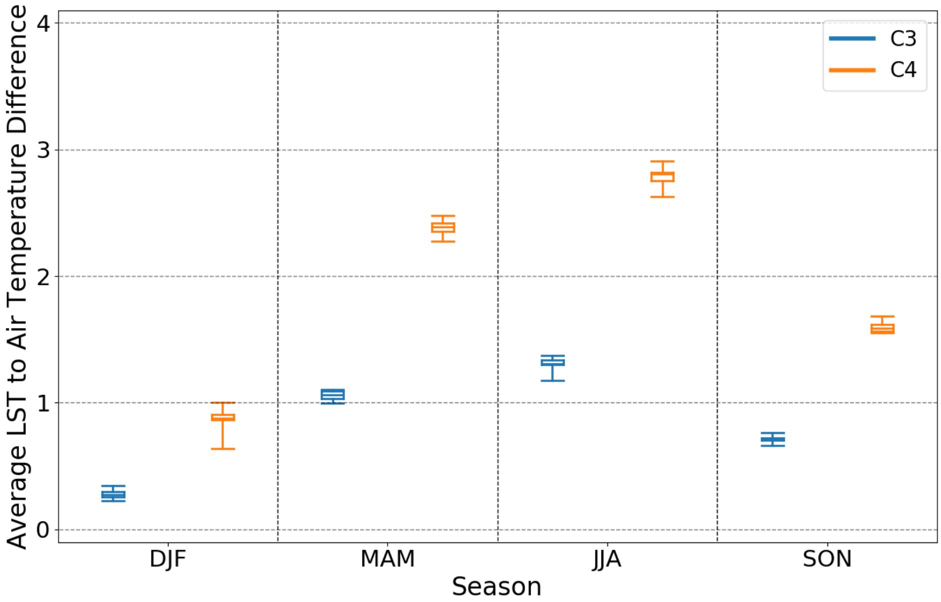

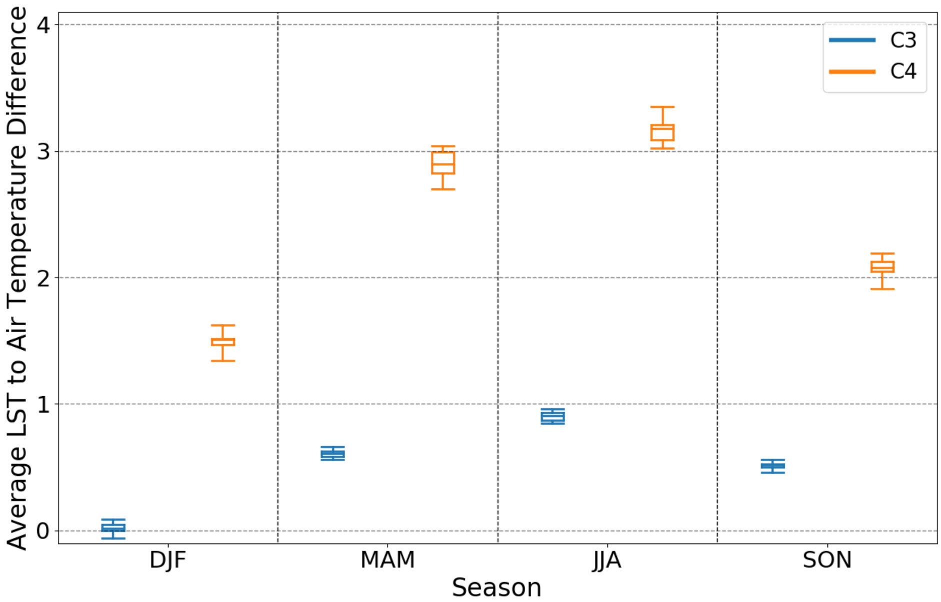

Figure 3-1 Seasonal mean variations in model LST-T2m (°C) for areas dominated by C3 (blue) and C4 (orange) grass or crops across China (upper) and North America (lower). Boxes show the 25th and 75th percentiles, with the line in the box representing the median value. The whiskers show the minimum and maximum values of the variation across all years 2003-2014 inclusive (within the region).

3.2 Evaluation of LST_cci MODIS products against ground data at the Valencia Test Site (R. Niclòs, University of Valencia)

3.2.1 Key Messages

- TERRA_MODIS_L2P / AQUA_MODIS_L2P and TERRA_MODIS_L3C / AQUA_MODIS_L3C LST_cci products were evaluated against ground data at the Valencia Test Site to test accuracies for meteorological and climate studies within the University of Valencia's research projects.
- Evaluations for the MODIS operational LST products (MOD/MYD11_L2 and MOD/MYD21) were also developed using the same ground data as reference data.
- The TERRA_MODIS_L2P / AQUA_MODIS_L2P products (and also the TERRA_MODIS_L3C / AQUA_MODIS_L3C products) systematically overestimate (around 4 K) ground LSTs, also leading root-mean-square differences (RMSD) of around 4 K.
- These overestimates were not observed for the MODIS operational products, with RMSDs of around 1.5K.
- Ones the overestimation will be solved, the LST_cci products will offer a good tool for climate studies.

3.2.2 Scientific Analysis

3.2.2.1 Aims of the study

TERRA_MODIS_L2P / AQUA_MODIS_L2P and TERRA_MODIS_L3C / AQUA_MODIS_L3C products (i.e., MODIS LST_cci 1 km and 5 km products both for EOS-Terra and EOS-Aqua overpasses, respectively) were evaluated against ground data at the Valencia Test Site [RD-29, RD-30] to test the accuracies of these Land Surface Temperature (LST) products for meteorological and climate studies within the research projects leaded by the University of Valencia (e.g., project CGL2015-64268-R (MINECO/FEDER, UE)). The Valencia Test Site is a uniform and thermally-homogeneous rice paddy area, with very different land covers due to the crop phenology across the year: water surfaces (in case of flooded soils), full vegetation cover and bare soils.

The MODIS operational products (MOD/MYD11_L2 and MOD/MYD21) were also evaluated using the same ground data as reference data for comparison. These products are obtained with the generalized split-window (SW) algorithm [RD-31, RD-32] and temperature-emissivity separation (TES) algorithms [RD-33, RD-34], respectively, and are disseminated through the NASA's Earth Data Search website (search.earthdata.nasa.gov).

The objective was also to contribute, with feedback to the LST_cci project, to generate more accurate LST products for climate applications.

3.2.2.2 Method

Ground TIR measurements were performed using several hand-held Cimel Electronique CE-312 radiometers. Measurements were acquired along predetermined transects over the test site and concurrently with MODIS overpasses in cloud-free conditions. The number of radiometers ranged from 2 to 4 depending on the day. Radiometers were calibrated in the laboratory (each year) and within international campaigns, so the calibration uncertainty was estimated [RD-35, RD-36].

The ground measurements were acquired following the methodology described in [RD-29] for cloud-free days from 2016 to 2018 (daytime only). The CE-312 radiometers measured the surface radiance within a spectral band *i*, $\boldsymbol{L_{surf,i}}$, which depends on the surface emissivity, $\boldsymbol{\varepsilon_i}$, as follows:

$$\textbf{Equation 3-1} \quad \boldsymbol{L_{surf,i} = \varepsilon_i B_i(T) + (1-\varepsilon_i) L_i{}^{\downarrow}{}_{a,hem}}$$

where $\boldsymbol{B_i(T)}$ is the channel Planck's function for a temperature T (here T being the LST). $\boldsymbol{L_i{}^{\downarrow}{}_{a,hem}}$ is the atmospheric downwelling irradiance divided by π [RD-30]. $\boldsymbol{L_i{}^{\downarrow}{}_{a,hem}}$ was measured using an Infragold Reflectance Target (IRT-94-100) made by Labsphere [RD-37], which is a highly diffuse gold panel with a reflectivity close to 0.92 in the 8 – 14 µm region.

Additionally, emissivities for the different land covers were measured at the site, and not assumed or estimated from threshold methods or databases. Emissivity measurements were taken using the TES method [RD-33, RD-38] applied to the ground data measured by the CE-312 radiometers and also the Box Method [RD-30].

The reference ground LSTs were obtained as the average of the LST measurements performed by all ground radiometers within five minutes of each overpass time.

3.2.2.3 Results

This section shows the results of the evaluations of the abovementioned LST_cci and operational LST products using the described ground data as reference (Section 3.2.2.2). Table 3-1 and Table 3-2 show the statistical differences of the product LSTs minus ground LSTs in terms of bias, standard deviation (SD) and root-mean-square differences (RMSD). Table 3-1 shows the results for the EOS Aqua – MODIS products and Table 3-2 for the EOS Terra – MODIS products. Results are also shown in Figure 3-2 and Figure 3-3.

Table 3-1: Results of the evaluation of the day-time LST_cci and operational products for EOS Aqua - MODIS.

	LST_AQUA_MODIS_L2P – LST_ground (K)	LST_AQUA_MODIS_L3C – LST_ground (K)	LST_AQUA_MYD11 – LST_ground (K)	LST_AQUA_MYD21 – LST_ground (K)
BIAS	4.4	3.5	0.0	0.9
SD	1.7	1.1	0.9	1.2
RMSD	4.7	3.7	0.9	1.5
N. EVENTS	18	13	20	20

Table 3-2: Results of the evaluation of the day-time LST_cci and operational products for EOS Terra - MODIS.

	LST_TERRA_MODIS_L2P – LST_ground (K)	LST_TERRA_MODIS_L3C – LST_ground (K)	LST_TERRA_MYD11 – LST_ground (K)
BIAS	3.6	3.5	0.0
SD	1.4	2.2	1.6
RMSD	3.8	4.1	1.6
N. EVENTS	31	32	30

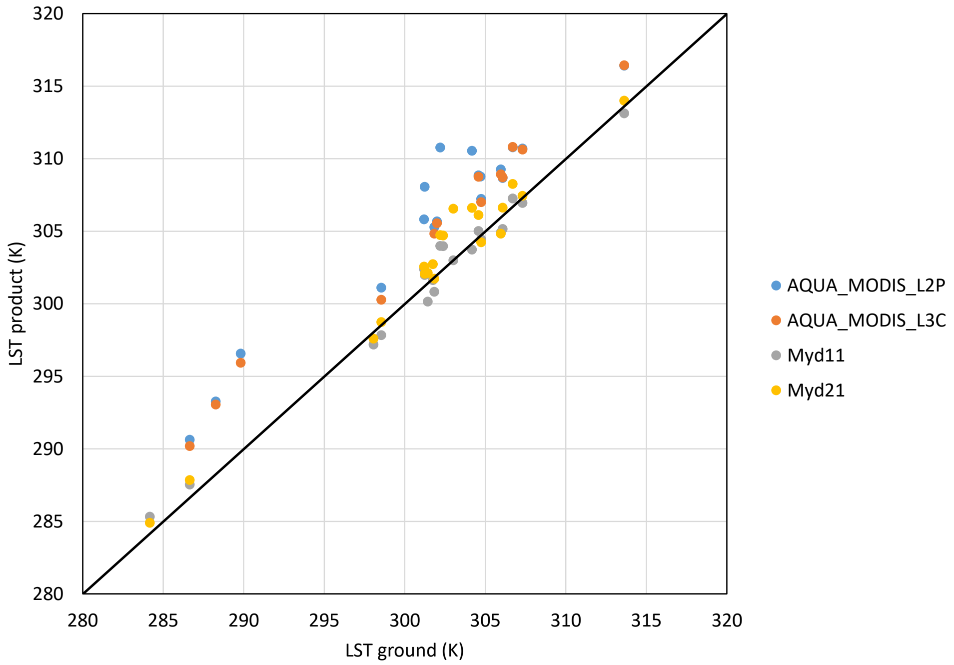

Figure 3-2: Comparison of LSTs obtained for the site coordinates the EOS Aqua – MODIS products (i.e., both the LST_cci AQUA_MODIS_L2P and AQUA_MODIS_L3C products and the MYD11 and MYD21 operational products) against ground LSTs. Results are shown for daytime only.

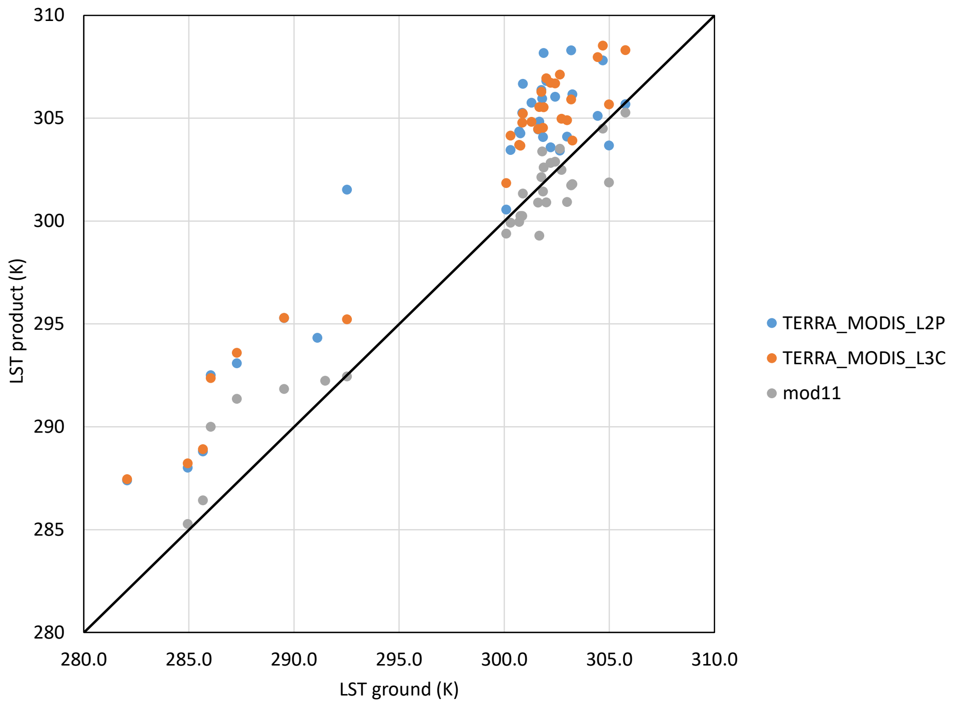

Figure 3-3: Comparison of LSTs obtained for the site coordinates by the EOS Terra – MODIS products (i.e., both the LST_cci TERRA_MODIS_L2P and TERRA_MODIS_L3C products and the MOD11 operational product) against ground LSTs. Results are shown for daytime only.

3.2.2.4 Conclusions

The results show that the LST_cci MODIS products overestimate ground LSTs (with bias and RMSD of around 4 K), both for LST_cci L2P and L3C products and also for EOS Aqua - MODIS and EOS Terra – MODIS. This overestimation was not observed for the operational products, neither in the case of the SW product (MYD/MOD11) nor in the case of the TES product (MYD/MOD21). The overestimates shown for these LST_cci products may be due to significant differences between the emissivities assigned for the site in the LST_cci products and ground-measured emissivities, which varied in the evaluation dataset because of land cover type changes at the site across the year.

3.2.3 Feedback on scientific utility of the LST_cci products

A few sentences summarising the experience with the LST_cci products in this study:

- products were accessible and easy to use since they were provided in NetCDF format, which is easily readable by several image processing software packages and programming languages.
- low spatial resolution for evaluation purposes in the case of L3C products.
- LST_cci products for other satellite sensors (e.g., MetOp-A/B/C AVHRR/3 and S-NPP/JPSS1 VIIRS) could be also interesting, as well as more availability of information about the algorithms, specific techniques and data used to generate the LST_cci products.

3.3 Reports from other users

A further seven other known users have requested access to LST_cci data. All these users were contacted and asked for feedback (in any format) on their experiences so far. Only one user has responded to say that they had downloaded a few data files but had not progressed further than this with any analysis. This user reported they had no issues with getting hold of the data and loading into Python, etc. As a non-expert in the use of satellite data, their main comment is that they found the directory structure quite confusing, with a lot of unexplained acronyms and recommended that a readme file for this beta data portal would be useful to help get them started.

4. Summary

This section synthesises the findings from the studies presented in Section 2 and Section 3 regarding the suitability of the beta LST_cci products for climate applications. The following sub-sections summarise the conclusions from the overall climate assessment by theme.

4.1 Data set accuracy, stability and precision

The accuracy, precision and stability of the LST_cci data sets is being assessed through a dedicated validation work stream within the LST_cci project and is reported elsewhere. However, three of the UCS and one other user study have compared the LST_cci data sets with other surface temperature observations that provide insight into the performance of these data: 1) LST anomalies from 0.05° L3 MODIS, ATSR-2, AATSR, SLSTR, and the MW and IR CDRs have been compared with collocated station T2m anomalies over Europe within the Met Office UCS, 2) MODIS L3 LST data (locally derived from MODIS L2 1km data) have been compared with airborne LST observations over Greenland in the DMI UCS, 3) collocated 0.01° L3 LSTs and station T2m observations have been compared at urban locations in Romania within the MeteoRomania UCS, and 4) MODIS L2 and L3 LST data have been compared with in situ LST observations over a site in Spain. The following conclusions are based on these studies:

- The behaviour of the LST_cci MODIS L3 products (0.01° and 0.05°) with respect to T2m over Europe is as expected based on the published literature (e.g. RD-03, RD-39]:
  - Actual temperatures and anomalies are well correlated ($r \approx 0.8$-0.9) and slopes (e.g. LST vs T2m) are reasonably close to unity ($m \approx 0.8$-1.0)
- The behaviour of the LST_cci MW L3 product (0.25°) over Europe with respect to T2m is as expected:
  - Anomalies are well correlated ($r \approx 0.8$) and slopes (e.g. LST vs T2m) are reasonably close to unity ($m \approx 0.8$)
- The behaviour of the LST_cci ATSR-2 and AATSR L3 products (0.05°) over Europe, including the IR multi-sensor product, with respect to T2m is slightly worse than expected:
  - Anomalies are only moderately well correlated ($r \approx 0.6$) and slopes (e.g. LST vs T2m) are considerably less than unity ($m \approx 0.6$).
  - The relatively poor performance of the ATSR-2/AATSR products, e.g. compared to MODIS, may be due to the smaller number of station-satellite matchups that are possible due to the narrower swath with the ATSR instruments.
- The LST_cci MODIS L2 (and possibly L3) data appear to be up to a few K too cold over the Greenland Ice Sheet. However, the pixel-to-pixel precision (or consistency) appears to be slightly better than for an equivalent AVHRR data set (not from LST_cci), although this AVHRR data set does not exhibit the cold offset observed in the MODIS data. There are also occasions where the MODIS data are 30-40 K too cold that do not look like typical cloud contamination, which may represent some error in the processing of these data in this region.

  There were known processing bugs in this version of the LST_cci MODIS processor, which have subsequently been addressed by the development team. This may be the cause of the observed 30-40 K cold outliers observed in this UCS. Systematic cloud contamination over ice sheets has also been observed by the Science Team, which will be addressed with the new cloud screening approach in v2.00.

- The LST_cci Aqua/Terra MODIS L2 and L3 data appear to be up to a few K too warm over a test site in Spain. This offset is not apparent in the operational NASA MODIS products and may be due to an incorrect surface emissivity being used in the LST_cci products.

  An updated emissivity data set is being implemented in v2.0 of the LST_cci MODIS products. The LST_cci v1.0 products are based on an older emissivity data set and it is expected that the updated version in v2.0 will improve the accuracy of the LST_cci retrievals in this case.

- The LST_cci multi-sensor L3 (0.05°) products show non-climatic discontinuities due to sensor changes and are therefore not suitable for applications that require data which are homogeneous with time (e.g. trend analysis).
  - The ATSR-2 period of the IR multi-sensor CDR appears to be noisier than the AATSR period, particularly for LST_{day}.
  - The LSTs from individual sensors that comprise the MW CDR appear to drift with time and there are jumps in the record at sensor transitions.

  It should be noted that the time difference correction in the beta version of the IR multi-sensor product was experimental and performed with respect to MODIS as a reference sensor. For this v1.0 product, sensor inter-calibration was not included, which has since shown to have an impact. Furthermore, subsequent analysis has suggested that there may be some drift in the MODIS channels, which is also being addressed. A modified approach will be implemented for the v2.0 product, which is expected to improve the homogeneity of the multi-sensor product significantly. Efforts are also underway to implement a correction for the temporal drift in the MW multi-sensor product, which should be included in the next version of the product.

- There are significant differences between the trends in the LST_cci single-sensor L3 (0.05°) product anomalies and the equivalent trends in T2m over Europe. Further investigation is needed to understand these differences before the data can be used for analysis of climatic trends (as the differences may be due to inhomogeneities in the LST_cci data sets).

4.2 Data set artefacts and issues

Some data set artefacts and issues have been identified in the beta versions of the LST_cci data sets through several of the UCS, which are summarised below.

- LST_cci L3 IR LSTs produced through averaging over multiple orbits are often not meaningful and should be replaced by LSTs averaged over a single timestamp/orbit, or by providing the specific observations for each observation time.
  - In the MODIS L3 products (and most likely the other IR L3 products), a clear decrease in the LST vs T2m correlation and slope with increasing latitude is observed due to increased noise in the data that results from this multi-orbit averaging process.
  - For many applications, LSTs without a specific observation time (e.g. because they are produced by averaging over multiple orbits/times) cannot be used.

  This will be addressed by the Science Team when producing version 2.00 of the products, where the L3 IR datasets will be based on the observations closest to the nominal overpass time of the sensor.

- There is significant residual cloud contamination in the LST_cci IR products.
  - This has been noted in particular for MODIS/Aqua, SEVIRI and ATSR-2 (India only), but all IR products suffer from this issue.

- If cloud screening cannot be improved, it would be useful to have some guidance for users on this issue.

Some of the residual cloud contamination in the MODIS data was due to a bug in the LST_cci processor, which has now been resolved. More generally, there is a dedicated project work package on improving cloud screening in LST_cci. A new probabilistic approach to cloud screening will be implemented for the next LST_cci MODIS and ATSR data release, which should reduce the cloud contamination further in these products. The reported issue over India in ATSR-2 will be investigated: It is a known issue that ATSR-2 does not have any data over Central Asia and India during the mission lifetime due to an in-flight switch-off so there should be no data here. There are no plans to update the cloud mask used in the LST_cci SEVIRI product, but the merged product will include an additional filtering mechanism.

4.3 Data file issues and recommendations

A number of issues relating to the data files themselves have been identified in the beta versions of the LST_cci data sets through several of the UCS, which are summarised below. This list also includes suggestions for other data-file improvements that have been requested by users.

- The current method for delivering LST_cci 0.01° is not optimal. Users of these data have had to spend considerable time mosaicking the data together.
  - It would be preferable if the data from each orbit were mosaiced beforehand and provided as tiles, similar to the gridded MOD11/MYD11 data products of NASA

Improved delivery of the 0.01° data is currently being investigated by the Science Team; a simple HxV system to identify the tiles according to their geolocation may be implemented.

- There are discrepancies between the IR and MW product formats. Having a more consistent format between the two product types is preferred. For example:
  - Classification is by day/night for IR but ascending/descending for MW.
  - Provision of quality flags / other information is inconsistent (e.g. no land cover class information is provided in the MW data and no quality flag is provided in the IR data).

Many users prefer day/night classification, which is why this approach has been adopted for the IR data sets. However, it is not possible to classify the MW observations in the same way because the overpass time is ~6-8 am/pm. The differences in quality flags between the two product types arise from the different processing requirements in each case. However, consultation with users will continue on both these points to find the best way forward in each case.

- There are some errors in the information provided in the data files:
  - Incorrect information in the global attribute 'platform' in the MULTISENSOR_IRCDR_L3S.
  - 'standard_name' field contents for both latitude and longitude is set to 'latitude' in the MODIS L3 products (and possibly other IR products).

Both these issues have already been resolved ready for the next product release.

- The current land cover class information provided in the LST_cci files is static; provision dynamic/annual land cover data would be better (note users do appreciate the provision of land cover class data in the LST_cci data files).
  Dynamic land cover information will be implemented for the next release of the LST_cci data files.

- Provision of satellite view zenith angles with sign (i.e. '-' or '+') that indicates whether the view is towards the east or west (it is noted that this will not be meaningful at very high latitudes but for the majority of the orbit this is useful information). This would be easier for users, who currently have to obtain this information from the satellite azimuth angle, which is an extra step.
- The latitude and longitude values of the LST_cci MODIS/ATSR 0.01° products global attributes "geospatial_lat_min", "geospatial_lat_max", "geospatial_lon_min", and "geospatial_lon_max" need to be corrected by half pixel in order to be equal to the actual bounding box coordinates of each LST image. The values currently provided are the latitudes and longitudes of the centre of the four corner pixels. This should be corrected.
- Uncertainty information in the LST_cci MSG_SEVIRI_L3U products is only available from mid-2008 onwards, and the first period of available data in the record on uncertainty give negative values.
- *This is a known processing bug and has been resolved for the next release.*
- The spatial extent of the SEVIRI disk changes at some point in the record, so only in the later part also north-eastern Europe and parts of south America have valid data. This should be rectified in some way, or at least a guidance note should be issued to users.
- The fields 'ncld' and 'variance' in the LST_cci MSG_SEVIRI_L3U products are included in the files but have no meaning as the values are instantaneous and nearest neighbour gridding was performed. As the LST_cci files have a standardised format across all products, it is suggested that a comment is added to inform the user of these unmeaningful fields for SEVIRI in the file attributes.
- For the LST_cci 0.01° products, naming the LST_cci data files indicating the geolocation of the data would be helpful, or providing them with a clear identification according to the MODIS tiling system or for example the Sentinel-2 tile grid (UTM system). This would make the identification of tiles containing the LST_cci data over the areas of interest easier.
- Provide a 'readme' file in the current public directory for the beta products that includes a list of acronyms and information on the directory structure.

4.4 Other recommendations / future considerations

The following recommendations to consider for future work were suggested in this assessment. It is recognised that many of these are beyond the scope of the current LST_cci project phase:

- Dedicated effort towards improving IST algorithms should be considered
- Extend SEVIRI data record beyond 2008-2010
- Implement a geometrical correction to 'adjust' the LSTs to nadir-equivalent LSTs for all sensors
- *For the current LST_cci project phase, a geometrical correction will only be implemented for the merged product.*
- Provide downscaled (higher spatial resolution) SEVIRI data (e.g. downscaled with MODIS)
- Provide instantaneous LSTs in L3 products as an extra fields in the LST_cci products (e.g averaged LSTs over each orbit separately).
- Provide infilled LST products where IR data have been used.
- Provide LST products for AVHRR/3 and VIIRS.

In addition, it is noted that the uptake of uncertainty information in UCS and other studies is minimal so effort should focus on improving this in the user community. Many of the studies require spatial and/or temporal averaging of the data and therefore require propagation of uncertainty information, which is a non-trivial task. (It takes some weeks or even months to write robust software to re-grid data and propagate uncertainties correctly, which is a major barrier to users.) The project should consider providing tools or example software to propagate uncertainties in the LST_cci data sets.

4.5 Feedback from CCI Science Team

The User Case Studies have provided highly relevant feedback for the Science Team to improve the performance of the LST_cci products. However, it is worth noting that the climate assessment reported here has been performed on the very first beta products generated early in Phase I of LST_cci. These were very similar to the pre-cursor GlobTemperature products, and for the most part focussed on MODIS. The Science Team have in parallel been working on improvements to these products for the next data version (V2.00), and have taken on-board feedback from the CRG studies throughout the progress of the Use Case Studies. These improvements are yet to be made available to the UCS teams, but will be accessible early in Year 3 of Phase I.

While the focus of this report is on an independent climate assessment of the LST_cci products it is useful to provide the wider context of how the project is responding to the feedback through close interaction with the CRG. Some of the key advances that are being implemented in V2.00 of the LST_cci products, in response to the majority of the UCS feedback, are summarised below and presented in detail in [RD-40]:

- Cloud masking:
  - This has been reported as an issue by the majority of UCS teams and is particularly emphasised for the MODIS product. Evidence suggests this is a result of two different factors:
    - Use of the operational MODIS cloud mask rather than the new CCI Probabilistic cloud mask which is being implementing across polar-orbiting IR sensors in V2.00
    - Some processing bugs in V1.00 have come to light following early user feedback, with some months having very bad cloud masking. These bugs have been fixed for in V2.00
  - Cloud screening is being improved for the CDRs also in a dedicated Work Package.
- Propagation of L2P to L3C products:
  - Multiple UCS have found that the averaging of multiple orbits per day at high latitudes have caused issues with usability for climate and loss of timing information from lower level data.
  - In V2.00 the IR datasets will not average these orbits, and instead will take the observations closest to the nominal overpass time. This will maintain the original acquisition time and thus ensure traceability.
- Systematic warm and cold biases in MODIS data:
  - The operational MODIS use the latest emissivity retrievals either direct from multi-channels or indirect from new emissivity data sources. The LST_cci MODIS V1.00 product uses an old emissivity dataset. This difference in input emissivity data is the hypothesised cause of the systematic biases.
  - This has been changed in V2.00 such that MODIS will use the newest CAMEL data which was originally generated from MOD21 and ASTER inputs.

- Systematic cloud contamination is seen in offline tests over ice sheets by the Science Team, and is the likely source of the cold bias for these regions. This is being addressed with the new cloud making approach for V2.00

- Stability:
  - Work by the Science Team have identified [RD-1] temporal drifts in calibration for each MODIS instrument and for each channel of these instruments. Intercalibration corrections are being implemented in V2.00 and should improve the stability of the MODIS products.
  - For the ATSR CDR, a time difference correction was implemented in V1.00 which was experimental and performed with respect to MODIS as a reference sensor. No account was made of the inter sensor calibration, which has been shown since to have an impact. It is expected that V2.00 will show an improvement.
- Data usage:
  - The IR data follows a day / night split for the L3C products. This is consistent with Sea Surface Temperature CCI and this will be maintained for LST_cci.
  - Quality flags are only provided in the L3C products for the MW product. This is because these provide additional indication of sub-optimal retrievals. In contrast, the IR data processing for Level-3 has already filtered out all the problem data, such as cloudy pixels or low confidence pixels, and so the quality level is already expected to be at its highest.
  - Incorrect global attributes reported have been fixed in V2.00
  - Several studies have commented on the difficulty in dealing with the customised L3C data. In V2.00 global L3C data at 0.01° will be made available with use of a simple H x V tiling system under consideration.
  - In V1.00 land cover was a static auxiliary input dataset. In V2.00 a dynamic approach has been implemented using annual Land Cover CCI as the basis.
  - A correction to nadir-like retrievals is being implemented in the Merged Product.
  - There are however some changes that will not be implemented, since they would be in contradiction with the community established approaches first set out in GlobTemperature and brought forward into LST_cci:
    - Satellite zenith angles will still be provided as per V1.00. Viewing direction can be acquired already via the satellite azimuth variable.
    - The geolocation values provided will continue to be the latitudes and longitudes of the centre of the grid-cells.
    - Suggested downscaling of coarse resolution SEVIRI data is out-of-scope in Phase 1 of LST_cci.

End of document